

Potent Arylsulfonamide Inhibitors of Tumor Necrosis Factor- α Converting Enzyme Able to Reduce Activated Leukocyte Cell Adhesion Molecule Shedding in Cancer Cell Models

Elisa Nuti,[†] Francesca Casalini,[†] Stanislava I. Avramova,[†] Salvatore Santamaria,[†] Marina Fabbi,^{*,‡} Silvano Ferrini,[‡] Luciana Marinelli,[§] Valeria La Pietra,[§] Vittorio Limongelli,[§] Ettore Novellino,[§] Giovanni Cercignani,^{||} Elisabetta Orlandini,[†] Susanna Nencetti,[†] and Armando Rossello^{*,†}

[†]Dipartimento di Scienze Farmaceutiche, Università di Pisa, via Bonanno 6, 56126 Pisa, Italy, [‡]Istituto Nazionale per la Ricerca sul Cancro, Largo R. Benzi 10, 16132 Genova, Italy, [§]Dipartimento di Chimica Farmaceutica e Tossicologica, Università di Napoli "Federico II", Via Domenico Montesano 49, 80131 Napoli, Italy, and ^{||}Dipartimento di Biologia, Unità di Biochimica, Università di Pisa, Via San Zeno, 51, 56127 Pisa, Italy

Received December 18, 2009

Activated leukocyte cell adhesion molecule (ALCAM) plays a relevant role in tumor biology and progression. Our previous studies showed that ALCAM is expressed at the surface of epithelial ovarian cancer (EOC) cells and is released in a soluble form by ADAM-17-mediated shedding. This process is relevant to EOC cell motility and invasiveness, which is reduced by nonspecific inhibitors of ADAM-17. For this reason, ADAM-17 may represent a new useful target in anticancer therapy. Herein, we report the synthesis and biological evaluation of new ADAM-17 inhibitors containing an arylsulfonamidic scaffold. Among the new potential inhibitors, two very promising compounds **17** and **18** were discovered, with a nanomolar activity for ADAM-17 isolated enzyme. These compounds proved to be also the most potent in inhibiting soluble ALCAM release in cancer cells, showing a nanomolar activity on A2774 and SKOV3 cell lines.

1. Introduction

A disintegrin and metalloproteinases (ADAMs)^a are zinc endopeptidases belonging to the large superfamily of metzincins and are strictly related to matrix metalloproteinases (MMPs). In fact, they are type I transmembrane proteins that contain a metalloprotease and a disintegrin-like domain.¹

ADAM-17 or tumor necrosis factor- α converting enzyme (TACE) is a member of the ADAM family involved in the cleavage of several substrates that are relevant to cancer progression.² Among these are included epidermal growth factor receptor (EGFR) ligands,³ which are activated by proteolytic cleavage, and several cell adhesion molecules (CAMs) of the immunoglobulin superfamily.⁴

Activated leukocyte cell adhesion molecule (ALCAM or CD166) belongs to the subgroup with five extracellular immunoglobulin-like domains (VVC₂C₂C₂). As a CAM, it

plays key roles in homeostasis and cellular architecture in the body, being involved in cell–cell and cell–matrix interactions. In fact, ALCAM mediates cell–cell clustering through homophilic (ALCAM–ALCAM) and heterophilic (ALCAM–CD6) interactions⁵ and its transmembrane and cytoplasmic domains anchor ALCAM to the actin, thus connecting it to cytoskeleton mobility.^{6,7} Various observations indicate that ALCAM plays a relevant role in tumor biology and progression.⁸ During cancer development, complex adhesive interactions acting in concert with activation of proteolytic cascades determine cell release from the primary tumor and promote invasiveness.^{9,10} The overexpression or de novo expression of ALCAM at the cell surface can promote cell adhesion and clustering.^{6,11} These observations have a direct correlation in several human tumors, including melanoma, prostate, breast, bladder, and colorectal cancer, where noticeable alterations in expression of ALCAM have been reported.¹² Our previous studies, conducted by means of an anti-ALCAM recombinant antibody (scFv I/F8), showed that ALCAM is expressed at the surface of epithelial ovarian cancer (EOC) cells, can be internalized following soluble ligand engagement,¹³ and is released in a soluble form (sALCAM) by ADAM-17-mediated shedding.¹⁴ This process is relevant to EOC cell motility, which is reduced by nonspecific inhibitors of ADAM-17¹⁴ such as **1** (CGS 27023A).¹⁵ Moreover, clinical correlation data indicated that the decreased membrane expression of ALCAM is a marker of poorer outcome in EOC patients, suggesting a role of ADAM-17 in EOC.¹⁶ Other studies showed that ADAM-17 cleaves not only ALCAM but also desmoglein-2 (Dsg-2), a component of intercellular desmosome junctions,¹⁷ and L1-CAM.¹⁸ Activation of the EGFR leads to the up-regulation of

^{*}To whom correspondence should be addressed. For A.R.: phone, +39 050 2219562; fax, +39 050 2219605; E-mail: aros@farm.unipi.it. For M.F.: phone, +39 010 5737377; fax, +39 010 5737374; E-mail, marina.fabbi@istge.it.

^a Abbreviations: ADAM, a disintegrin and metalloproteinase; MMP, matrix metalloproteinase; TACE, tumor necrosis factor- α converting enzyme; EGFR, epidermal growth factor receptor; CAM, cell adhesion molecule; ALCAM, activated leukocyte cell adhesion molecule; EOC, epithelial ovarian cancer; Dsg-2, desmoglein-2; MMPI, MMP inhibitor; sALCAM, soluble ALCAM; TIMP, tissue inhibitor of metalloproteinase; ZBG, zinc-binding group; NMM, *N*-methylemorpholine; DIPEA, *N,N*-diisopropylethylamine; DIAD, diisopropyl azodicarboxylate; DMAP, 4-(dimethylamino)pyridine; EDC, *N*-(3-Dimethylaminopropyl)-*N'*-ethylcarbodiimide hydrochloride; TFA, trifluoroacetic acid; SAR, structure–activity relationship; PV, pervanadate; ELISA, enzyme-linked immunosorbent assay; EGF, epidermal growth factor; TK, tyrosine kinase; MTT, 3-(4,5-dimethylthiazol-2-yl) 2,5-diphenyltetrazolium bromide; APMA, *p*-aminophenylmercuric acetate.

ADAM-17 activity and to the shedding of adhesion molecules,¹⁹ allowing increased tumor cell mobilization. Altogether, these findings reveal an essential role of ADAM-17 in the shedding of cell–cell adhesion molecules. Because loss of cell adhesion by CAMs has been implicated in tumor progression, ADAM-17 may therefore represent an useful target in anticancer therapy.^{14,17,20}

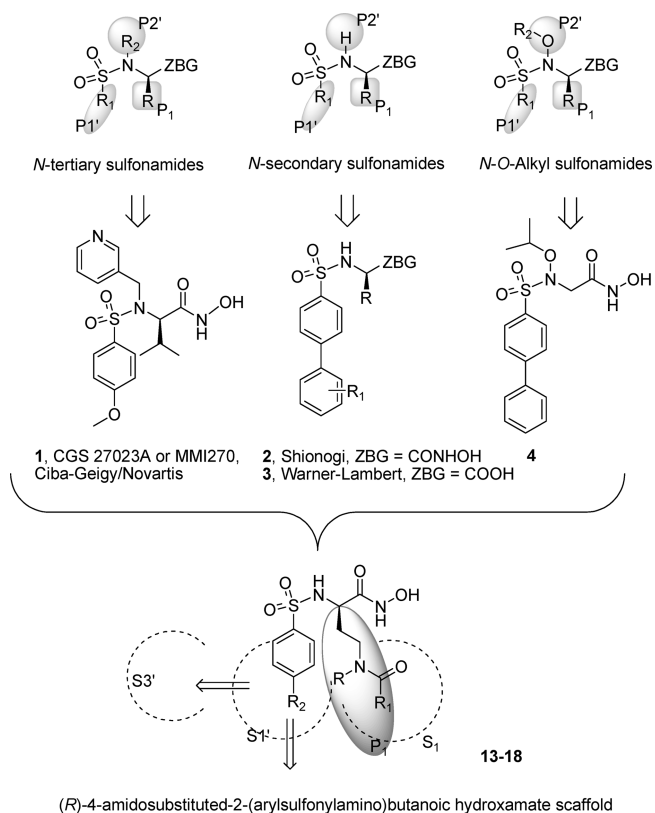


Figure 1. Evolution of the new scaffold of ADAM-17 inhibitors.

Table 1. In Vitro Enzymatic^a and Cellular^b Activities of Early Inhibitors **4–12** and the Reference Compound **1**

| compd | R | R ₁ | R ₂ | enzyme assay, IC ₅₀ (nM) | | | | | cell assay, inhibition % ^c of constitutive sALCAM release in A2774 ^d (10 μM) |
|-----------|---------------|----------------|----------------|-------------------------------------|------|------|-------|--------|--|
| | | | | MMP1 | MMP2 | MMP9 | MMP14 | ADAM17 | |
| 4 | <i>O</i> -iPr | H | Ph | 12000 | 12 | 200 | 2300 | 120000 | 0 |
| 5 | <i>i</i> -Bu | H | Ph | 4800 | 12 | 34 | 530 | 53000 | 14 |
| 6 | H | H | Ph | 610 | 2.0 | 34 | 70 | 2400 | 35 |
| 7 | <i>O</i> -iPr | H | OMe | 110000 | 5000 | 4100 | 9500 | 180000 | 0 |
| 8 | <i>i</i> -Bu | H | OMe | 300 | 13 | 4.8 | 13 | 2300 | 26 |
| 9 | H | H | OMe | 3000 | 32 | 130 | 210 | 1800 | 32 |
| 10 | H | H | Br | 270 | 40 | 290 | 360 | 3900 | 13 |
| 11 | <i>O</i> -iPr | <i>i</i> -Pr | OMe | 1100 | 190 | 170 | 240 | 10000 | 0 |
| 12 | <i>i</i> -Bu | <i>i</i> -Pr | OMe | 56 | 29 | 7.2 | 16 | 1100 | 9 |
| 1 | | | | 56 | 25 | 4.8 | 23 | 160 | 33 |

^a Enzymatic data are mean values for three independent experiments performed in duplicate. ^b Whole cells assays were performed and tested in duplicates. One representative experiment of three independent ones is shown. SD were generally within ±10%. ^c Percent inhibition observed at 10 μM concentration of the test compounds. ^d A2774 is a human epithelial ovarian cancer cell line.

At the beginning of our studies, to prove which metallo-proteinases could be involved in ALCAM shedding, we used a small panel of synthetic MMP inhibitors (MMPIs). In particular, we first studied the effect of the use of different sulfonamido-based MMPIs²¹ on sALCAM release. These inhibitors belong to the well-known families of tertiary sulfonamides (such as **1**, by Ciba-Geigy/Novartis), secondary sulfonamides (such as **2**,²² by Shionogi and **3**,²³ by Warner Lambert Company), and tertiary *N*-*O*-alkyl sulfonamides (such as **4**²⁴) (Figure 1). The last one is a more recently described family of sulfonamides highly selective on some MMPs and therefore potentially useful in this study.²⁵

The human EOC cell line A2774, which displays high ALCAM levels, was used as a starting model. The inhibitory potency and selectivity toward some selected MMPs vs ADAM-17 was compared to the inhibition of sALCAM release by whole cells following treatment with synthetic hydroxamate-based MMPIs²⁶ belonging to the three classes cited above (Table 1). For this preliminary evaluation, some secreted MMPs, such as collagenase-1 (MMP-1), gelatinase-A and -B (MMP-2 and MMP-9), and the membrane bound MT1-MMP (MMP-14) were selected together with ADAM-17. These MMPs are overexpressed in many tumors and are responsible for some other key functions in this pathology.²⁷

Regarding the inhibitors, compounds **4–12** (Table 1), which presented classical substituents able to drive potency and selectivity toward these MMPs and ADAM-17 on their P1 (R₁), P1' (R₂), and P2' (R) positions, were chosen and compared with the reference compound **1**. Secondary sulfonamides **6**²⁸ and **9**¹⁵ were equipotent to **1** in the cell assay on constitutive sALCAM release, with inhibition ranging between 32 and 35% at the tested dose (10 μM). The tertiary sulfonamides, compounds **5**,²⁴ **8**,¹⁵ and **12**, resulted in being less potent with respect to the secondary ones, with 9–26% inhibition on sALCAM release. The tertiary *N*-*O*-alkyl sulfonamides, such as **4** and its analogues **7**²⁴ and **11**, devoid of any activity on ADAM-17, resulted in being completely inactive

Table 2. In Vitro Enzymatic^a and Cellular^b Activities of Synthesized Derivatives **13–19** and the Reference Compound **1**

| compd | R | R ₁ | R ₂ | enzyme assay, IC ₅₀ (nM) | | | | | | cell assay, IC ₅₀ (nM) |
|-----------|--------------|---|------------------------------------|-------------------------------------|------|------|-------|--------|---------------------|--|
| | | | | MMP1 | MMP2 | MMP9 | MMP14 | ADAM17 | ADAM10 ^c | inhibition of sALCAM release ^d in A2774 |
| 13 | H | (CH ₂) ₂ NHCOCH ₃ | Ph | 196 | 0.70 | 8.6 | 34 | 300 | nd | 960 |
| 14 | H | (CH ₂) ₂ Pht | 2-CF ₃ -Ph | 5000 | 390 | 430 | 1800 | 44000 | nd | > 10000 |
| 15 | H | (CH ₂) ₂ NHCOCH ₃ | Br | 1500 | 190 | 190 | 300 | 110 | 2300 | 1400 |
| 16 | H | (CH ₂) ₂ Pht | Br | 4.0 | 1.5 | 1.1 | 0.9 | 210 | nd | 2900 |
| 17 | H | (CH ₂) ₂ NHCbz | OCH ₂ CCCH ₃ | 1100 | 17 | 46 | 210 | 1.6 | 240 | 11 |
| 18 | H | (CH ₂) ₂ Pht | OCH ₂ CCCH ₃ | 350 | 4.2 | 3.5 | 4.3 | 0.70 | 190 | 15 |
| 19 | <i>i</i> -Bu | (CH ₂) ₂ Pht | OCH ₂ CCCH ₃ | 400 | 21 | 13 | 29 | 59 | 2000 | 570 |
| 1 | | | | 56 | 25 | 4.8 | 23 | 160 | 890 | 380 |

^a Enzymatic data are mean values for three independent experiments performed in duplicate. ^b Whole cells assays were performed and tested in duplicates. One representative experiment of three independent ones is shown. SD were generally within $\pm 10\%$. ^c For assays on ADAM10 were used substrate concentrations 5-fold higher than those used for the other enzymes. ^d Inhibition of pervanadate-induced sALCAM release. nd: not determined.

also in the cell-based assay assessing sALCAM release. As it can be seen from these preliminary data, the increase of inhibitory activity on ADAM-17, going from *N*-*O*-alkyl sulfonamides to tertiary sulfonamides, to secondary sulfonamides, follows the increase of inhibition % of sALCAM release by the ALCAM-expressing A2774 cells, thus suggesting the involvement of ADAM-17 in ALCAM shedding. See for example activity of hydroxamates **4**, **5**, and **6** (IC₅₀ on ADAM-17: 126000, 53000, 2400 nM, corresponding to inhibition of constitutive sALCAM release of 0, 14, and 35%, respectively) and of **7**, **8**, and **9** (IC₅₀ on ADAM-17: 184000, 2300, 1790 nM, corresponding to inhibition of constitutive sALCAM release of 0, 26, and 32%, respectively).

This first result allowed us to hypothesize ADAM-17 as the metalloproteinase involved in ALCAM shedding. In fact, in following studies, we showed that sALCAM release is completely inhibited by the presence of recombinant tissue inhibitor of metalloproteinase 3 (rTIMP-3), a well-known biological ADAM-17 inhibitor, but not of rTIMP-1 and rTIMP-2.¹⁴ Finally the use of specific siRNA and in vitro digestion allowed us to formally demonstrate that ALCAM is a substrate of ADAM-17.^{14,29} In addition, Bech-Serra et al.,¹⁷ using cells genetically deficient for ADAM-10 or ADAM-17, demonstrated that ALCAM ectodomain shedding is severely impaired only in the absence of the latter. Altogether, these data suggested that sALCAM release may be controlled by ADAM-17 activity. Because the ADAM-17-mediated cleavage of CAMs is a relevant step in cancer cell motility, and the use of an unselective MMP/ADAM inhibitor, such as **1**, reduced ALCAM shedding from cancer cell lines, in this paper we sought to use sALCAM release as a novel biological read-out system on tumor cell cultures to investigate new MMP/ADAM-17 inhibitors, in conjunction with classical in vitro assays on purified enzyme.

Considering the structural differences in S1 and S1'–S3' pockets between the selected MMPs and ADAM-17 and the best results obtained with the secondary sulfonamides, we decided to develop new secondary sulfonamido-based inhibitors more active on ADAM-17 with the aim to enhance the

inhibition of ALCAM shedding in a metalloproteinase-dependent cancer cell system. Therefore, starting from our previous studies³⁰ on the effects of the P1–P3' substitution and bearing in mind the literature in this field,³¹ we designed, synthesized and tested new ADAM-17 inhibitors, **13–19** (Figure 1). All these compounds are characterized by a common (*R*)-4-amidosubstituted-2-(arylsulfonylamino)butanoic hydroxamate moiety able to interact differently with the S1/S1' and/or S1/S1'–S3' subsites of these different families of enzymes, modulating potency and selectivity based on their terminal residues R–R₂.

Other scientists³² in the past years have disclosed some α -aminoacid-based sulfonamide hydroxamates as inhibitors of MMPs and ADAM-17 in the treatment of inflammatory diseases (such as rheumatoid arthritis and osteoarthritis), which are somewhat similar to compounds **13–19**.³³ Nevertheless, this is the first reported systematic study of the use of ADAM-17 inhibitors on shedding of a CAM in cancer cell models. Finally, molecular modeling studies were carried out to reveal the potential interactions that govern the recognition and the binding of the best inhibitor **17** to the ADAM-17 enzyme and to rationalize the structure–affinity relationships of the novel ADAM-17 inhibitors at the molecular level.

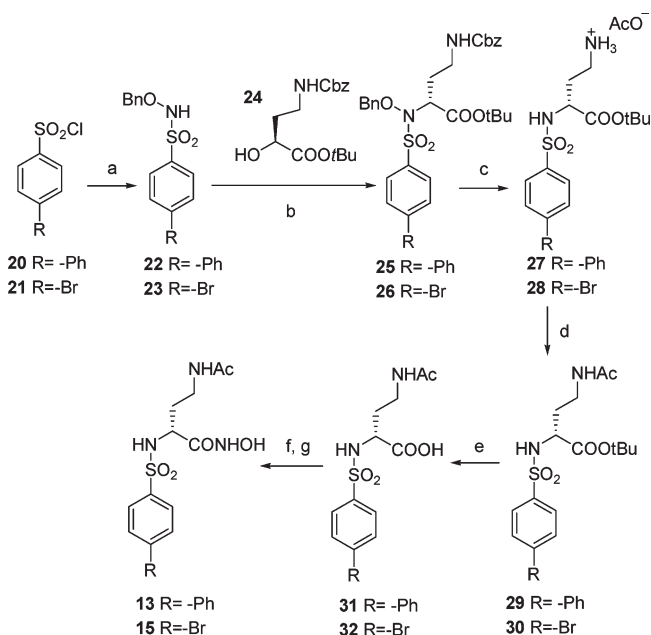
2. Chemistry

Sulfonamide hydroxamic acids **13** and **15** (Table 2) were prepared as shown in Scheme 1. Biphenyl-4-sulfonyl chloride **20** and 4-bromobenzenesulfonyl chloride **21** reacted with *O*-benzyl-hydroxylamine hydrochloride in the presence of *N*-methylmorpholine (NMM) to afford protected sulfonamides **22** and **23**. A Mitsunobu condensation of sulfonamides **22**, **23** with α -hydroxy-*tert*-butyl ester **24**,^{25a} gave *tert*-butyl esters **25**, **26**. Acetamido derivatives **29** and **30** were obtained by Pd-catalyzed hydrogenation of **25**, **26**, followed by acetylation with acetyl chloride, using *N,N*-diisopropylethylamine (DIPEA) as base. Acid cleavage of esters **29**, **30** yielded carboxylates **31**, **32**, which were condensed with *O*-(*tert*-butyldimethylsilyl)hydroxylamine and finally deprotected

with trifluoroacetic acid (TFA) to give hydroxamic acids **13** and **15**.³⁴

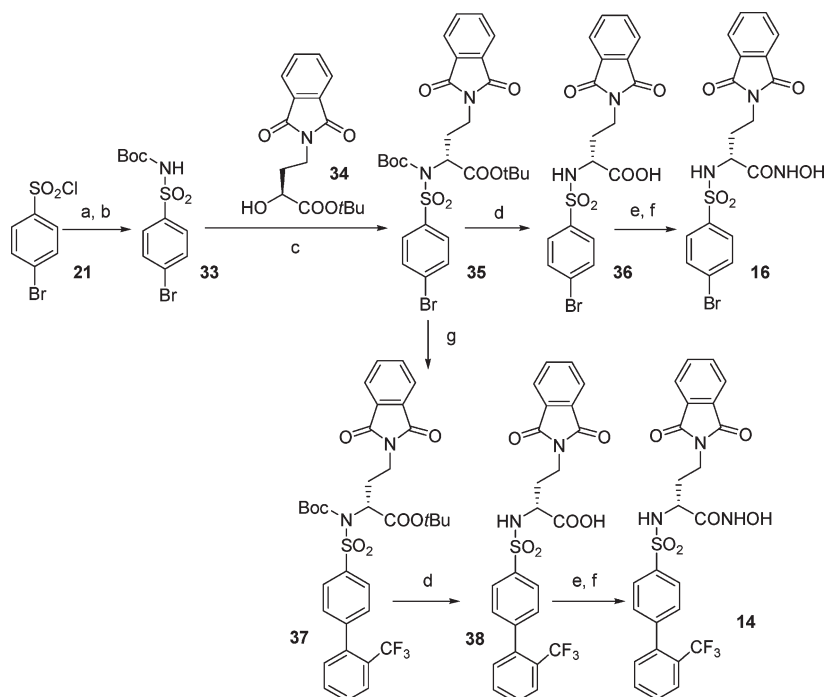
Hydroxamates **14** and **16** (Scheme 2) were obtained starting from 4-bromobenzenesulfonyl chloride **21**, which was converted into the corresponding Boc-sulfonamide **33** by reaction with ammonia aq solution followed by treatment with di-(*tert*-butyl)dicarbonate in CH₂Cl₂ using 4-(dimethylamino)-

Scheme 1. Synthesis of Compounds **13**, **15**^a



^a Reagents and conditions: (a) BnONH₂·HCl, NMM, THF; (b) PPh₃, DIAD, THF; (c) H₂, Pd/C 10%, MeOH, AcOH; (d) acetyl chloride, DIPEA, DMF; (e) TFA, CH₂Cl₂, 0 °C; (f) TBDMSiONH₂, EDC, CH₂Cl₂; (g) TFA, CH₂Cl₂, 0 °C.

Scheme 2. Synthesis of Compounds **14**, **16**^a

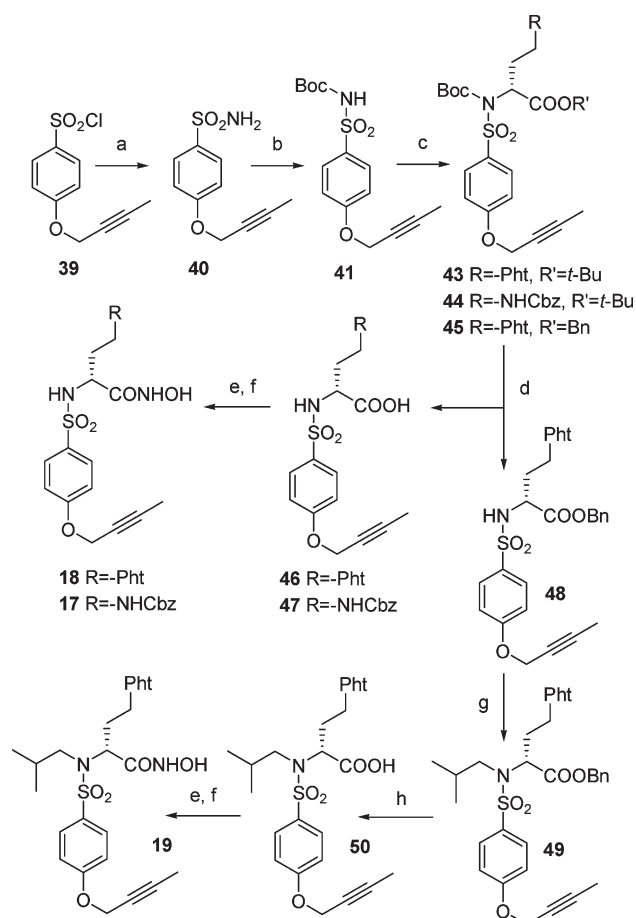


^a Reagents and conditions: (a) NH₃ aq, CH₃CN, 0 °C to rt; (b) (Boc)₂O, Et₃N, DMAP, CH₂Cl₂; (c) PPh₃, DIAD, THF; (d) TFA, CH₂Cl₂, 0 °C; (e) TBDMSiONH₂, EDC, CH₂Cl₂; (f) TFA, CH₂Cl₂, 0 °C; (g) 2-(trifluoromethyl)phenylboronic acid, Pd(PPh₃)₄, K₃PO₄, H₂O, dioxane, 85 °C.

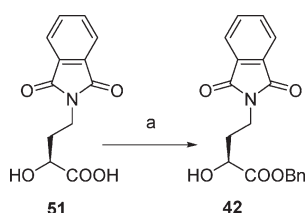
pyridine (DMAP) as acylation catalyst.³⁵ This conversion was carried out because *N*-(sulfonyl)carbamates are useful *N*-nucleophiles in the Mitsunobu reaction, which was employed subsequently to afford *tert*-butyl ester **35** from Boc-sulfonamide **33** and the previously described optically active alcohol **34**.³⁰ Acid hydrolysis of **35** yielded the *NH*-sulfonamide carboxylate **36**, which was finally converted into the corresponding hydroxamate **16** by condensation with *O*-(*tert*-butyldimethylsilyl)hydroxylamine and acid cleavage by TFA. The aryl bromide intermediate **35** was also converted into diaryl derivative **37** by Pd-catalyzed Suzuki³⁶ coupling with 2-(trifluoromethyl)phenylboronic acid in the presence of K₃PO₄. Acid cleavage of **37** yielded carboxylic acid **38**, which was finally converted in its corresponding hydroxamate **14** as described above.

The butynyloxy-based sulfonamide hydroxamates **17–19** (Scheme 3) were synthesized starting from 4-butyloxybenzenesulfonyl chloride **39**, obtained using a literature procedure.³⁷ **39** was converted into the corresponding Boc-sulfonamide **41** by reaction with ammonia, followed by treatment with di-(*tert*-butyl)dicarbonate. Sulfonamide **41** underwent Mitsunobu reaction in the presence of diisopropyl azodicarboxylate (DIAD) and triphenylphosphine with optically active alcohols **34**, **24**, and **42** to give respectively the esters **43–45** of (*R*) configuration. While *tert*-butyl esters **43** and **44** were deprotected by treatment with TFA and finally converted into the corresponding *NH*-sulfonamide hydroxamates **18** and **17**, benzylic ester **45** was deprotected and then *N*-alkylated by treatment with 1-iodo-2-methylpropane in DMF using cesium carbonate as base. Subsequently, *N*-isobutyl derivative **49** was submitted to alkaline hydrolysis to give carboxylate **50**, which was converted in the tertiary sulfonamide hydroxamate **19** as described above.

Finally, in Scheme 4 is reported the synthesis of (*S*)- α -hydroxy ester intermediate **42**. α -Hydroxy acid **51** was easily

Scheme 3. Synthesis of Compounds 17–19^a

^a Reagents and conditions: (a) NH₃ aq, CH₃CN, 0 °C to rt; (b) (Boc)₂O, Et₃N, DMAP, CH₂Cl₂; (c) alcohol **34** or **24** or **42** (see Scheme 4), PPh₃, DIAD, THF; (d) TFA, CH₂Cl₂, 0 °C; (e) TBDM-SiONH₂, EDC, CH₂Cl₂; (f) TFA, CH₂Cl₂, 0 °C; (g) 1-iodo-2-methyl propane, K₂CO₃, DMF; (h) KOH, H₂O, 80 °C.

Scheme 4. Preparation of (S)-α-Hydroxy Ester **42**^a

^a Reagents and conditions: (a) BnBr, Cs₂CO₃, DMF, 0 °C to rt.

turned into benzyl ester **42** by reaction with benzyl bromide in the presence of cesium carbonate in DMF.

3. Results and Discussion

Biological Activity on Isolated Enzymes. The newly synthesized hydroxamates **13**–**19** were tested *in vitro* for their ability to inhibit human recombinant ADAM-17 and MMP-1, MMP-2, MMP-9, and MMP-14, by a fluorometric assay using **1** as reference compound (Table 2). The panel of enzymes was extended to ADAM-10 (known also as mammalian kuzbanian protein) on the basis of the recently discovered roles of the couple ADAM-10 and ADAM-17 on carcinogenesis.^{20,38}

As shown in Table 2, the introduction of an amidic chain in the (*R*)-configuration in P1 strongly affected the affinity of

the inhibitors for ADAM-17, causing a marked increase of activity. In fact, compound **13** bearing an *N*-ethylacetamidic chain in P1 resulted in being 10-fold more active than its unsubstituted analogue **6** (Table 1), showing an IC₅₀ = 300 nM despite the presence of a biphenyl group in P1' that is quite unsuitable to fit the S1' pocket of ADAM-17. In fact, it is well-known from literature³⁹ that the S1' pocket of this enzyme is rather narrow and is connected to S3' region through a distinctive bend that allows access to the large pocket. The replacement of the biphenyl group of compound **13** with a 4-bromobenzene substituent (compound **15**) caused only a 3-fold increase of activity against ADAM-17 (IC₅₀ = 110 nM). Compound **15** resulted as potent as the reference compound **1** on ADAM-17, being more selective over MMPs and in particular over MMP-1 (IC₅₀ = 1500 nM) and MMP-14 (IC₅₀ = 300 nM). To further increase activity on ADAM-17 of this class of inhibitors, we introduced other different chains in P1, like those previously used for the synthesis of MMPs inhibitors.³⁰ Compound **16**, having an *N*-ethylphthalimidic chain in place of the *N*-ethylacetamidic group of **15**, displayed a strong increase of activity on the tested MMPs and a slight decrease of potency toward ADAM-17. Derivative **14**, with the same alkyl chain in α to the hydroxamate and a 2-CF₃-biphenyl group in P1', resulted a poor inhibitor of both ADAM-17 and MMPs probably because of the excessive bulkiness of the P1' substituent.

It has been shown by Levin et al.³⁷ that incorporation of a 4-(but-2-ynyloxy)benzene group as the P1' substituent on the sulfonamide-based inhibitors was able to increase potency on ADAM-17. Hence, we decided to incorporate a butynyloxy substituent at the P1' position of this class of molecules to improve activity on ADAM-17. As expected, propargylic derivatives **17** and **18** were found to be better ADAM-17 inhibitors than *para*-bromo derivatives **15** and **16**. In particular, compound **18**, bearing an *N*-ethylphthalimidic chain in P1, resulted the most potent inhibitor of the series, with an IC₅₀ = 0.70 nM on ADAM-17. Compound **17**, which differs from **18** only for the P1 chain (R₁ = CH₂CH₂NHCbz), displayed a similar activity toward ADAM-17 (IC₅₀ = 1.6 nM) and was more selective than **18** over MMP-14 and MMP-1.

As expected, secondary sulfonamides resulted more active on ADAM-17 with respect to their corresponding *N*-alkylated sulfonamides, as can be seen comparing compound **18** with **19** (IC₅₀ = 59 nM), which presented an isobutyl group on sulfonamide nitrogen.

From this brief SAR study, it appears that both P1' and P1 substituents are important in determining ADAM-17 affinity, and the best results were obtained summing up the effects of a butynyloxy group in P1' and an *N*-ethylamidic chain in P1. Thus, this optimization process led to the discovery of two nanomolar inhibitors of ADAM-17, compound **17** and **18**, which showed also a good activity on ADAM-10 (IC₅₀ = 240 and 190 nM, respectively).

Biological Activity on Cancer Cell Lines. The activity of the newly synthesized ADAM-17 inhibitors **13**–**19** was then evaluated in living cancer cells. Initially, the study was performed on human EOC cell lines (A2774 and SKOV3) and then extended to other cell types (breast cancer lines MCF7 and MDA-MB-468 and neuroblastoma cell line GI-CA-N). All cell lines expressed high levels of ALCAM at the cell surface, as assessed by immunofluorescence, expressed ADAM-17 proenzyme and mature forms, as assessed by

Western blot, and released ALCAM in soluble form both constitutively and following activation by tyrosine kinase receptors.^{14,29} Modulation of sALCAM release, which is easily assessed in cell culture conditioned media by ELISA assay, was therefore chosen as read-out test to score the ADAM-17 inhibitory activity of the various compounds in living cells. First of all, the compounds were tested on A2774 cells, which constitutively shed the highest levels of sALCAM among a panel of EOC cell lines (data not shown). Each compound was assessed at 10 μ M, 1 μ M, 100 nM, and 10 nM concentrations in duplicate cultures with overnight incubation to test constitutive sALCAM release (not shown). In the case of treatment with pervanadate, PV was added 30 min after the inhibitors and incubation carried out for an additional 90 min (Figure 2). The sALCAM levels,

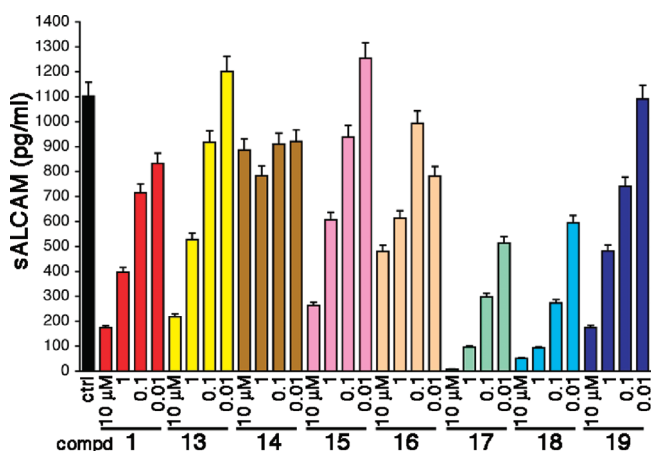


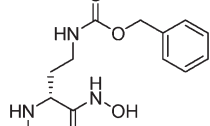
Figure 2. Inhibition of pervanadate-induced sALCAM release. Supernatants from A2774 EOC cells cultured with PV in the presence of the indicated amounts of the different MMPis were assessed by ELISA for sALCAM. The amount of sALCAM detected in conditioned medium from cells treated with solvent (DMSO) and PV (black column) was used as 100% shedding control. Whole cells assays were performed and tested in duplicates. One representative experiment is shown.

measured by ELISA, were compared to control cultures treated with the corresponding amounts of DMSO solvent (Figure 2).

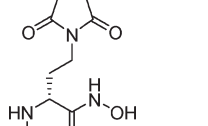
Table 2 shows the inhibition of pervanadate-induced sALCAM release on A2774 cells by compounds **13–19** and the reference compound **1** in comparison with activity against isolated enzymes. As already seen for early MMP inhibitors (Table 1), the ability of the new hydroxamates to reduce ALCAM shedding had a similar pattern to potency on ADAM-17 inhibition. The introduction of the butynyl-oxy group in P1', which increased activity on ADAM-17, led also to an enhanced potency in cell assay. In fact, the propargylic derivatives **17** and **18** resulted the best of the series both on enzymatic and cell assay with an IC_{50} = 11 and 15 nM on A2774 cells, respectively. Compound **19**, the *N*-tertiary sulfonamide analogue of **18**, had a 40-fold drop in activity on cells (IC_{50} = 570 nM) comparable to the 80-fold decrease shown in ADAM-17 inhibition probably due to the presence of the isobutyl substituent in P2'. Finally, compounds **17** and **18** were also from 100- to 230-fold more potent on ADAM-17 and about 30-fold more potent on cells with respect to the reference compound **1**, which had an IC_{50} of 160 nM on the isolated enzyme and of 380 nM on A2774 cell line.

Whole cells display a wide repertoire of metalloproteases that could variably interact with a given compound, contributing to its overall effect. Each cell line, expressing an individual pattern of metalloproteases, could then behave differently either qualitatively or quantitatively as different dose-response. Therefore, we tested the two compounds which best inhibited sALCAM release by A2774 cells on other cancer cell lines. Table 3 shows the inhibitory activity of **17** and **18** toward constitutive sALCAM release measured on the five ALCAM-expressing cancer cell lines described above. Moreover, data from the literature suggest that in some cell types inducible ectodomain shedding is linked to ADAM-17 activity, whereas constitutive shedding may result from redundant proteolysis.^{18,19,40} The new inhibitors activity was therefore tested in the presence of tyrosine

Table 3. In Vitro Cellular Activity^a of Synthesized compounds **17**, **18** and the Reference Compound **1**



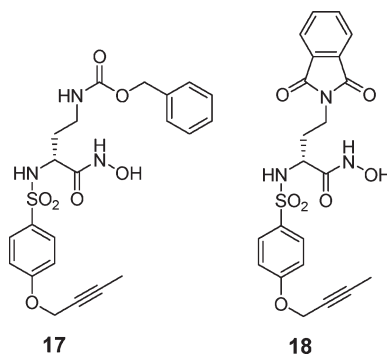
17



18

| inhibition of sALCAM release, IC ₅₀ (nM) | | | | | | | | | | | | | |
|---|---------------------|--------------------|------------------|---------------------|------------------|---------------------|--------------------|------------------|---------------------|--------------------|------------------|---------------------|--------------------|
| compd | A2774 | | | SKOV3 | | MCF7 | | | MDA-MB-468 | | | GICAN | |
| | const. ^b | perv. ^c | EGF ^d | const. ^b | EGF ^d | const. ^b | perv. ^c | EGF ^d | const. ^b | perv. ^c | EGF ^d | const. ^b | perv. ^c |
| 17 | 260 | 11 | 890 | nd | 3.2 | 1600 | 53 | 420 | 420 | 1100 | 110 | 90 | 500 |
| 18 | 1100 | 15 | 550 | 2600 | 4.3 | 1400 | 51 | 760 | 1700 | 800 | 280 | 97 | 73 |
| 1 | 18000 | 380 | 3200 | 13000 | 110 | 6900 | 750 | 3000 | 1400 | 10000 | 750 | 4400 | 1100 |

^aWhole cells assays were performed and tested in duplicates. SD were generally within $\pm 10\%$. One representative experiment of three independent ones is shown. ^bInhibition of constitutive sALCAM release. ^cInhibition of pervanadate-induced sALCAM release. ^dInhibition of EGF-induced sALCAM release. nd: not determined.



kinase activation. Two stimuli were chosen, one broad and one specific. Pervanadate is a general phosphotyrosine phosphatase inhibitor whose final effect is to increase the tyrosine phosphorylation of many intracellular proteins and to activate multiple signal transduction pathways, which lead to metalloproteinases activation.⁴¹ Epidermal growth factor (EGF) is a known EOC growth factor acting through a TK receptor,⁴² which has been shown to up-regulate ADAM-17¹⁷ and to increase ALCAM shedding.¹⁴ Whichever cell line was tested, **17** and **18** performed better than the reference compound **1**, maintaining good inhibitory properties on ALCAM shedding in any condition (under pervanadate/EGF stimuli or constitutive). In particular, the inhibitory effects were more evident on A2774 pervanadate-stimulated, on SKOV3 EGF-stimulated, and on GICAN nonstimulated cells, where **17** and **18** were able to reduce ALCAM shedding in the low nM range (IC₅₀ between 3.2 and 97 nM). In the same experiments, compound **1** resulted markedly less active, with IC₅₀ values 2 orders of magnitude higher. Moreover, compounds **17** and **18** used at 1 μ M concentration almost completely blocked PV-induced sALCAM shedding in A2774 EOC cells (Figure 2), suggesting that in this experimental setting ADAM-17 activity is not redundant.

Cell morphology was monitored by microscopy, and no toxicity was detected on parallel cultures by MTT assay (data not shown).

4. Molecular Modeling

Molecular modeling was performed with the aim of revealing the potential interactions that govern the recognition and the binding of the best inhibitor **17** to the ADAM-17 enzyme and to rationalize the here-presented structure–affinity relationships (SARs) at the molecular level. Compound **17** was chosen because it has an activity comparable to **18**, both in enzymatic assay on isolated ADAM-17 and in A2774 cell assay, accompanied with a better selectivity over MMPs (see data in Table 2).

In the attempt to overcome the rigidity of the enzymes during the inhibitor docking process, a detailed comparison among all the ADAM-17 X-ray structures currently available in the PDB was performed and those that were most diverse were selected for docking experiments (see paragraph “X-ray Structures Selection for Docking Studies” and Table 4 in Supporting Information for any details). Although this strategy, commonly used to include receptor flexibility during the docking process is still far from perfection, it did allow the exploitation of all crystallographic data collected to date on ADAM-17.

The automated docking calculations of **17** into the five selected ADAM-17 X-ray structures (PDB codes: 2I47,⁴³ 3EDZ,⁴⁴ 3EWJ,⁴⁵ 2DDF,⁴⁶ 2OI0⁴⁷) were performed using Glide 5.5 (Grid-based Ligand Docking with Energetics) in extra precision mode. Docking of **17** in the 3EWJ structure resulted in poorly ranked and not full convincing poses as the hydroxamate moiety is mostly found to not coordinate the catalytic zinc ion in the expected bidentate fashion. Moreover, the relatively small P1' group of **17**, which allocates itself in the S1' pocket does not engage strong interactions with the amino acids lining the pocket. This is probably due to the fact that in the 3EWJ structure, the enzyme has been cocrystallized with an inhibitor possessing a much more extended P1' group (2-phenyl-quinoline) with respect to **17**. As a consequence, the S1' loop rearranges its conformation to make room and to

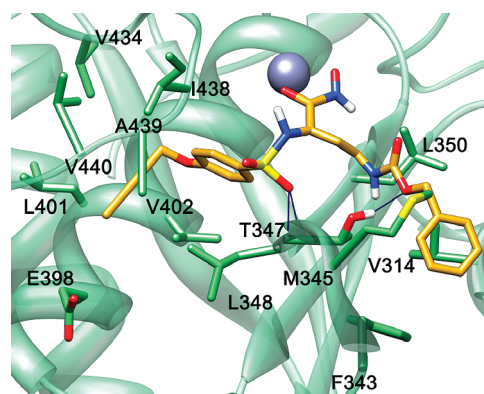


Figure 3. Preferred binding mode of **17** within the active site of ADAM-17 as resulted from docking calculations.

interact with such a peculiar inhibitor. Similar outcomes are obtained from docking experiments when 2OI0 is used.

Differently, docking results were pretty similar and more convincing with respect to the previous one when 2I47 and 3EDZ structures were used. Particularly, as shown in Figure 3, the hydroxamate group chelates the zinc ion in a bidentate fashion, while the butynyloxy group is well inserted in the S1' pocket where multiple hydrophobic contacts were detected with V434, V402, A439, L401, and L348 side chains and with E398 β - and γ -carbons. Moreover, one sulfonamide-oxygen establishes the commonly found bifurcated H-bond with L348 and Gly349 backbone NH. The benzyl-carbamate moiety lies along the S1 pocket interacting with the L350, V314, F343, and M345 side chains, and an H-bond is detected between the carbamate oxygen and T347 side chain.

Slight different results were obtained when the closed (2DDF) structure of ADAM-17 was used. Indeed, the Glide program suggests two different binding poses: the first one named “binding mode A” (Figure 4 in Supporting Information), which is totally similar to the previous one (obtained using 2I47 and 3EDZ) as regards the metal chelation and occupancy of the S1' pocket, but where the benzyl-carbamate moiety reaches out toward the S2 pocket, contacting the S355 β -carbon and forming a π – π interaction with the H409; the second one, named “binding mode B”, which is absolutely superimposable to the one obtained when 2I47 and 3EDZ structures were used. Thus, to elucidate the most probable binding pose (A and B) of **17**, two 10 ns MD simulations were performed by means of AMBER 9.0 package software to the two possible binary complexes calculated by the docking program. Results of MD simulations clearly indicate binding mode B as preferential orientation for **17**. Indeed, while MD simulation for mode A has shown that the benzyl-carbamate moiety of the inhibitor does not establish any stable interaction, waving between the S1, S2, and S3' walls pockets, MD simulation of mode B has shown that the same group remains stable in its position during all the simulation (see rmsd plots and Figure 6 in Supporting Information). The finding of a preferred binding conformation for **17** allows for a rationalization of the here-presented SAR data. Indeed, once more the inhibitory potency and the selectivity of action of the inhibitors is strongly influenced by the P1' and P1 groups. So, a bulky rigid straight P1' group (**13** and **14**) or vice versa a small moiety (**15** and **16**) leads to a low inhibitor activity toward ADAM-17, which possesses a deep and arched S1' pocket. On the contrary, the butynyloxy group (**17**–**19**) entirely plunges into the S1' pocket and adequately fills it. Moreover, in

ADAM-17 the S1 pocket is a shallow, solvent exposed, hydrophobic area. Thus, a rather long, flexible, hydrophobic P1 group would be able to fit into this area establishing multiple interactions with the side chains of the lining residues. Accordingly, the *N*-ethylacetamide (**15**), the *N*-ethylphthalimide (**16**, **18**, **19**), and the benzyl-ethylcarbamate (**17**) chains are all able to adjust in that cavity although **15** and **16** show lower inhibitory potencies due to the unproductive insertion of a bromine atom on the P1' group if compared to **17** and **18**, respectively. Finally, **19** shows a 84-fold decrease in ADAM-17 inhibition with respect to **18** due to the presence of a *N*-substituted sulfonamide, which would rearrange its conformation (probably loosing the bifurcated H-bond with L348 and Gly349 backbone) to avoid steric clashes with S1' loop backbone.

5. Conclusions

Considering the data coming from literature and our previous studies in this field, a series of (*R*)-4-amidosubstituted-2-(arylsulfonylamino)butanoic hydroxamates was designed and synthesized by exploiting the differences between MMP and ADAM-17 catalytic site. These compounds were evaluated as ADAM-17 inhibitors on isolated enzyme by a fluorometric assay and successively were tested in living cancer cells expressing ALCAM for they capacity to block sALCAM release. Among the novel analogues, two very promising compounds were discovered, **17** and **18**, which showed nanomolar activity for ADAM-17 and a good selectivity over MMP-1 and MMP-14. The same compounds resulted the most potent of the series on several cancer cell lines, inhibiting soluble ALCAM release better than the reference compound **1**. In particular, the inhibitory effects were more evident on A2774 pervanadate-stimulated, on SKOV3 EGF-stimulated and on GICAN nonstimulated cells, where **17** and **18** were able to reduce ALCAM shedding in the low nM range (IC₅₀ between 3.2 and 97 nM). No toxicity for these compounds was detected on parallel cultures by MTT assay. These preliminary results allowed us to validate ADAM-17/ALCAM pathway as new target in anticancer therapy. Compound **17** was chosen for further studies in in vivo cancer models and additional results will be reported in due course.

6. Experimental Section

Chemistry. Melting points were determined on a Kofler hot-stage apparatus and are uncorrected. ¹H and ¹³C NMR spectra were determined with a Varian Gemini 200 MHz spectrometer. Chemical shifts (δ) are reported in parts per million downfield from tetramethylsilane and referenced from solvent references. Coupling constants *J* are reported in hertz; ¹³C NMR spectra were fully decoupled. The following abbreviations are used: singlet (s), doublet (d), triplet (t), double-doublet (dd), broad (br), and multiplet (m). Where indicated, the elemental compositions of the compounds agreed to within ±0.4% of the calculated value. Chromatographic separations were performed on silica gel columns by flash column chromatography (Kieselgel 40, 0.040–0.063 mm; Merck) or using ISOLUTE Flash Si II cartridges (Biotage). Reactions were followed by thin-layer chromatography (TLC) on Merck aluminum silica gel (60 F254) sheets that were visualized under a UV lamp and hydroxamic acids were visualized with FeCl₃ aqueous solution. Evaporation was performed in vacuo (rotating evaporator). Sodium sulfate was always used as the drying agent. Commercially available chemicals were purchased from Sigma-Aldrich. The purity of the final compounds was determined by reverse-phase HPLC on a Merck Hitachi D-7000 liquid chromatograph.

HPLC purity was determined to be >95% for all final products using a Discovery C18 column (250 mm × 4.6 mm, 5 μm, Supelco), with a gradient of 40% water/60% methanol at a flow rate of 1.4 mL/min, with UV monitoring at the fixed wavelength of 242 nm. See the Supporting Information for compound purity analysis data for final compounds. Optical rotation were obtained on a Perkin-Elmer 343 polarimeter with a continuous Na lamp (589 nm).

General Procedure for the Synthesis of Sulfonamides 22, 23. A solution of the appropriate sulfonyl chloride **20**, **21** (31.32 mmol) in anhydrous THF (78.5 mL) was added dropwise to a stirred and cooled (0 °C) solution of *O*-benzylhydroxylamine hydrochloride (5.00 g, 31.32 mmol) and *N*-methylmorpholine (6.9 mL, 62.64 mmol) in anhydrous THF (78.5 mL). After stirring at RT for 3 days, the reaction mixture was diluted with EtOAc and washed with H₂O. The organic phase was dried over anhydrous Na₂SO₄, filtered, and evaporated under reduced pressure.

***N*-(Benzyloxy)biphenyl-4-sulfonamide (22).** The title compound was obtained from biphenyl-4-sulfonyl chloride **20** and benzylhydroxylamine hydrochloride following the general procedure. White solid (85% yield); mp 130–132 °C. ¹H NMR (CDCl₃) δ: 5.01 (s, 2H), 7.01 (s, 1H), 7.35 (m, 5H), 7.44–7.51 (m, 3H), 7.57–7.62 (m, 2H), 7.70–7.75 (m, 2H), 7.97–8.01 (m, 2H).

***N*-(Benzyloxy)-4-bromobenzenesulfonamide (23).** The title compound was obtained from 4-bromobenzenesulfonyl chloride **21** and benzylhydroxylamine hydrochloride following the general procedure. White solid (65% yield). ¹H NMR (CDCl₃) δ: 4.98 (s, 2H), 6.93 (br s, 1H), 7.35 (s, 5H), 7.63–7.64 (m, 1H), 7.68–7.69 (m, 1H), 7.75–7.76 (m, 1H), 7.79–7.80 (m, 1H).

General Procedure for the Synthesis of Esters 25, 26. DIAD (0.53 mL, 2.68 mmol) was added dropwise to a solution containing alcohol **24** (331 mg, 1.07 mmol), the appropriate sulfonamide **22**, **23** (1.61 mmol), and triphenylphosphine (843 mg, 3.21 mmol) in anhydrous THF (16.5 mL) under nitrogen atmosphere at 0 °C. The resulting solution was stirred for 4 h at RT and evaporated under reduced pressure.

***tert*-Butyl-(2*R*)-4-[(benzyloxy)carbonylamino]-2-[1,1'-(biphenyl-4-ylsulfonyl)-(benzyloxy)amino]butanoate (25).** The title compound was prepared from sulfonamide **22** and alcohol **24** following the general procedure. The crude was purified by flash chromatography on silica gel (*n*-hexane/EtOAc 3:1) to give a yellow oil (58% yield). ¹H NMR (CDCl₃) δ: 1.25 (s, 9H), 1.90–2.04 (m, 2H), 3.16–3.40 (m, 2H), 4.16 (t, *J* = 7.1 Hz, 1H), 4.93–5.00 (m, 1H), 5.07–5.19 (m, 4H), 7.33–7.37 (m, 10H), 7.41–7.59 (m, 5H), 7.66–7.70 (m, 2H), 7.92–7.97 (m, 2H). ¹³C NMR (CDCl₃) δ: 22.09, 27.87, 37.59, 62.75, 66.76, 80.87, 82.56, 127.43, 127.67, 128.16, 128.56, 128.72, 128.92, 129.14, 129.89, 129.94, 133.89, 134.80, 139.17, 146.84, 156.27.

***tert*-Butyl-(2*R*)-4-[(benzyloxy)carbonylamino]-2-[(4-bromobenzene-sulfonyl)-(benzyloxy)amino]butanoate (26).** The title compound was prepared from sulfonamide **23** and alcohol **24** following the general procedure. The crude was purified by flash chromatography on silica gel (*n*-hexane/EtOAc 3:1) to give a yellow oil (63% yield). ¹H NMR (CDCl₃) δ: 1.26 (s, 9H), 1.57–1.67 (m, 1H), 1.85–2.05 (m, 1H), 3.14–3.27 (m, 2H), 4.09 (t, *J* = 7.3 Hz, 1H), 4.95 (br s, 1H), 5.02–5.17 (m, 4H), 7.36 (s, 10H), 7.59–7.63 (m, 2H), 7.70–7.75 (m, 2H).

General Procedure for the Synthesis of Ammonium Salts 27, 28. A solution of the appropriate protected ester **25**, **26** (0.67 mmol) in MeOH (48 mL) was stirred under hydrogen atmosphere in the presence of 10% Pd–C (1:2 w/w) and glacial acetic acid (48 mL) for 17 h at RT. The resulting mixture was filtered on celite, and the filtrate was evaporated under reduced pressure.

(*R*)-3-(Biphenyl-4-ylsulfonamido)-4-*tert*-butoxy-4-oxobutan-1-aminium Acetate (27). The title compound was prepared from ester **25** following the general procedure. Clear oil (98% yield). ¹H NMR (CDCl₃) δ: 1.18 (s, 9H), 3.10–3.30 (m, 2H), 3.93 (br s, 1H), 5.0 (br s, 1H), 7.39–7.57 (m, 5H), 7.65–7.69 (m, 2H), 7.90–7.94 (m, 2H), 8.51 (br s, 1H).

(*R*)-3-(4-Bromophenylsulfonamido)-4-*tert*-butoxy-4-oxobutan-1-aminium Acetate (**28**). The title compound was prepared from ester **26** following the general procedure. Yellow oil (96.4% yield). ¹H NMR (DMSO-*d*₆) δ: 1.18 (s, 9H), 1.73–2.01 (m, 1H), 2.10 (d, 1H, *J* = 8 Hz), 2.74–2.89 (m, 2H), 3.84–3.90 (m, 1H), 7.29–7.34 (m, 1H), 7.47–7.86 (m, 3H), 8.15 (br s, 3H).

General Procedure for the Synthesis of Compounds 29, 30. A solution of the appropriate ammonium salt **27** or **28** (0.65 mmol) in dry DMF (6.75 mL) was treated with acetyl chloride (0.06 mL, 0.78 mmol) and *N,N*-diisopropylethylamine (0.23 mL, 1.30 mmol). The reaction mixture was stirred at RT for 17 h, then was diluted with EtOAc, washed with H₂O, dried over Na₂SO₄, and evaporated.

(*R*)-*tert*-Butyl 4-Acetamido-2-(biphenyl-4-ylsulfonamido)butanoate (**29**). The title compound was prepared from salt **27** following the general procedure. The crude oil was purified by flash chromatography on silica gel (*n*-hexane/EtOAc 3:2) to give a yellow oil (51% yield). ¹H NMR (CDCl₃) δ: 1.18 (s, 9H), 1.47–1.65 (m, 1H), 2.03 (s, 3H), 2.05–2.17 (m, 1H), 3.16–3.33 (m, 1H), 3.66–3.83 (m, 2H), 5.41 (d, *J* = 9.3 Hz, 1H), 6.27 (t, *J* = 5.5 Hz, 1H), 7.41–7.58 (m, 5H), 7.68–7.72 (m, 2H), 7.88–7.92 (m, 2H).

(*R*)-*tert*-Butyl 4-Acetamido-2-(4-bromophenylsulfonamido)butanoate (**30**). The title compound was prepared from salt **28** following the general procedure. The crude was purified by flash chromatography on silica gel (CH₂Cl₂/MeOH 98:2) to give a yellow oil (30% yield). ¹H NMR (CDCl₃) δ: 1.18 (s, 9H), 1.51–1.65 (m, 1H), 1.99 (s, 3H), 1.96–2.12 (m, 1H), 3.13–3.31 (m, 1H), 3.61–3.79 (m, 2H), 5.54 (d, *J* = 9 Hz, 2H), 6.29 (br s, 1H), 7.44–7.57 (m, 3H), 7.80–7.86 (m, 1H).

General Procedure for the Preparation of Carboxylic Acids 31, 32. TFA (0.55 mL, 7.17 mmol) was added dropwise to a stirred, ice-chilled solution of *tert*-butyl esters **29, 30** (0.12 mmol) in dry dichloromethane (1.0 mL). The mixture was stirred under these reaction conditions for 5 h and the solvent was removed in vacuo to give the carboxylic acids **31, 32**. The crude products were purified by trituration with *n*-hexane/Et₂O.

(*R*)-4-Acetamido-2-(biphenyl-4-ylsulfonamido)butanoic Acid (**31**). The title compound was prepared from ester **29** following the general procedure. Clear solid (84% yield). ¹H NMR (DMSO-*d*₆) δ: 1.57–1.70 (m, 2H), 1.72 (s, 3H), 3.00 (dd, 2H, *J*₁ = 6 Hz, *J*₂ = 13.2 Hz), 3.80 (dd, 1H, *J*₁ = 8.8 Hz, *J*₂ = 14.2 Hz), 7.39–7.56 (m, 3H), 7.72–7.84 (m, 7H), 8.24 (d, *J* = 8.8 Hz, 1H).

(*R*)-4-Acetamido-2-(4-bromophenylsulfonamido)butanoic Acid (**32**). The title compound was prepared from ester **30** following the general procedure. Brown solid (77.4% yield). ¹H NMR (acetone-*d*₆) δ: 1.77–1.97 (m, 2H), 1.86 (s, 3H), 3.03–3.24 (m, 1H), 3.29–3.48 (m, 1H), 3.98 (dd, *J*₁ = 7 Hz, *J*₂ = 15 Hz, 1H), 6.92 (d, *J* = 9 Hz, 1H), 7.20 (br s, 1H), 7.51–7.63 (m, 3H), 7.85–7.89 (m, 1H).

General Procedure for the Synthesis of Hydroxamates 13, 15. 1-[3-(Dimethylamino)propyl]-3-ethyl carbodiimide hydrochloride (EDC) was added portionwise (25 mg, 0.13 mmol) to a stirred and cooled solution (0 °C) of the appropriate carboxylic acid **31, 32** (0.087 mmol) and *O*-(*tert*-butyldimethylsilyl)hydroxylamine (12.8 mg, 0.087 mmol) in dry CH₂Cl₂ (2.2 mL). After stirring at room temperature overnight, the mixture was washed with water and the organic phase was dried and evaporated in vacuo.

Silyl precursors (0.05 mmol) were then dissolved in dry CH₂Cl₂ (0.4 mL) and TFA (0.22 mL, 2.8 mmol) was added dropwise at 0 °C. After 5 h of stirring, TFA was evaporated. The crude products were purified by trituration with *n*-hexane/Et₂O to give the desired hydroxamates **13** and **15**.

(*R*)-4-Acetamido-2-(biphenyl-4-ylsulfonamido)-*N*-hydroxybutanamide (**13**). The title compound was prepared from carboxylic acid **31** following the general procedure. *O*-Silylate derivative was purified by flash chromatography on silica gel (*n*-hexane/EtOAc 1:3) to give a yellow solid (60% yield). ¹H NMR (CDCl₃) δ: 0.02 (s, 6H), 0.85 (s, 9H), 1.85–2.00 (m, 2H), 2.05 (s,

3H), 3.00–3.10 (m, 1H), 3.49–3.63 (m, 1H), 3.69–3.81 (m, 1H), 6.19 (d, *J* = 7.7 Hz, 1H), 6.37 (t, *J* = 7.1 Hz, 1H), 7.41–7.60 (m, 5H), 7.67–7.71 (m, 2H), 7.85–7.89 (m, 2H), 10.39 (s, 1H).

Hydroxamic acid **13** was obtained as white solid (87% yield) after trituration with Et₂O; mp 193–195 °C. ¹H NMR (DMSO-*d*₆) δ: 1.43–1.67 (m, 2H), 1.72 (s, 3H), 2.87 (dd, *J*₁ = 6.9 Hz, *J*₂ = 13.1 Hz, 2H), 3.61 (dd, *J*₁ = 7.3 Hz, *J*₂ = 15.2 Hz, 1H), 7.43–7.55 (m, 3H), 7.69–7.76 (m, 3H), 7.84 (s, 4H), 8.19 (d, *J* = 8.4 Hz, 1H), 8.90 (br s, 1H), 10.59 (s, 1H). ¹³C NMR (CD₃OD-*d*₄) δ: 23.30, 27.72, 33.96, 46.71, 127.89, 129.31, 136.45, 138.62, 139.67, 168.53, 170.22. Anal. (C₁₈H₂₁N₃O₅S) C, H, N.

(*R*)-4-Acetamido-2-(4-bromophenylsulfonamido)-*N*-hydroxybutanamide (**15**). The title compound was prepared from carboxylic acid **32** following the general procedure. *O*-Silylate intermediate was obtained as a yellow oil (57% yield). ¹H NMR (CDCl₃) δ: 0.01 (s, 6H), 0.87 (s, 9H), 1.86–2.01 (m, 2H), 2.01 (s, 3H), 3.02–3.15 (m, 1H), 3.43–3.61 (m, 1H), 3.72–3.79 (m, 1H), 6.25 (br s, 1H), 6.55 (br s, 1H), 7.45–7.60 (m, 3H), 7.81–7.84 (m, 1H), 10.44 (br s, 1H).

Hydroxamic acid **15** was obtained as brown solid (95% yield) after trituration with Et₂O; mp 81–83 °C. ¹H NMR (DMSO-*d*₆) δ: 1.40–1.68 (m, 2H), 1.73 (s, 3H), 2.75–2.90 (m, 2H), 3.58 (dd, *J*₁ = 7 Hz, *J*₂ = 15 Hz, 1H), 7.56 (m, 2H), 7.76 (m, 2H), 8.09–8.14 (d, *J* = 9 Hz, 1H), 10.54 (br s, 1H). ¹³C NMR (CD₃OD-*d*₄) δ: 23.14, 35.21, 36.45, 36.58, 53.47, 127.93, 130.07, 133.55. Anal. (C₁₂H₁₆BrN₃O₅S) C, H, N.

tert-Butyl 4-Bromophenylsulfonfylcarbamate (**33**). Aqueous ammonia (7.5 mL) was added dropwise to a stirred, ice-chilled solution of sulfonyl chloride **21** (6.00 g, 23.48 mmol) in acetonitrile (2.35 mL). The resulting mixture was stirred for 10 min at RT, and then it was diluted with water and extracted with EtOAc. Organic layers were dried over Na₂SO₄ and concentrated in vacuo to give the 4-bromobenzenesulfonamide as a white solid (5.13 g, 92% yield). ¹H NMR (DMSO-*d*₆) δ: 7.47 (br s, 2H), 7.72–7.76 (m, 2H), 7.78–7.83 (m, 2H).

4-Bromobenzenesulfonamide (2.43 g, 10.3 mmol) was then suspended in dry CH₂Cl₂ (12.88 mL) containing DMAP (125.84 mg, 1.03 mmol) and Et₃N (1.59 mL, 11.33 mmol). A solution of di-(*tert*-butyl)dicarbonate (2.587 g, 11.85 mmol) in dry CH₂Cl₂ (20.62 mL) was added dropwise, and the reaction was stirred at room temperature overnight. The solution was concentrated in vacuo, and the residue was treated with EtOAc and HCl 1N. The organic phase was then washed with water and brine, dried over Na₂SO₄, and evaporated. The crude product was purified by flash chromatography on silica gel (*n*-hexane/EtOAc 4:1) using a Isolute Si (II) cartridge (Biotage) to give **33** as a white solid (2.65 g, 76% yield). ¹H NMR (CDCl₃) δ: 1.40 (s, 9H), 7.27 (br s, 1H), 7.69–7.71 (m, 2H), 7.87–7.91 (m, 2H).

(*R*)-*tert*-Butyl 2-(4-bromo-*N*-(*tert*-butoxycarbonyl)phenylsulfonamido)-4-(1,3-dioxoisindolin-2-yl)butanoate (**35**). DIAD (0.32 mL, 1.64 mmol) was added dropwise to a solution containing alcohol **34** (500 mg, 1.63 mmol), the protected sulfonamide **33** (550 mg, 1.63 mmol), and triphenylphosphine (1.2 g, 4.6 mmol) in anhydrous THF (16.4 mL) under nitrogen atmosphere at 0 °C. The resulting solution was stirred for 4 h at RT and evaporated under reduced pressure. The crude product was purified by flash chromatography on silica gel (*n*-hexane/EtOAc 5:1) to give **35** as a foamy solid (477 mg, 46% yield). ¹H NMR (CDCl₃) δ: 1.38 (s, 9H), 1.43 (s, 9H), 2.21–2.36 (m, 1H), 2.53–2.71 (m, 1H), 3.90 (t, *J* = 7.14 Hz, 2H), 4.99–5.06 (t, *J* = 7.0 Hz, 1H), 7.63–7.75 (m, 4H), 7.83–7.91 (m, 4H).

(*R*)-2-(4-Bromophenylsulfonamido)-4-(1,3-dioxoisindolin-2-yl)-butanoic Acid (**36**). Carboxylic acid **36** was prepared from ester **35** following the procedure previously described for **31**. Trituration with *n*-hexane gave **36** as a white solid (220 mg, 98% yield). ¹H NMR (DMSO-*d*₆) δ: 1.74–1.89 (m, 1H), 1.99–2.06 (m, 1H), 3.56–3.64 (m, 2H), 3.77–3.88 (m, 1H), 7.65–7.76 (m, 4H), 7.84 (s, 4H), 8.41–8.46 (m, 2H).

(*R*)-2-(4-Bromophenylsulfonamido)-4-(1,3-dioxoisindolin-2-yl)-*N*-hydroxybutanamide (**16**). Hydroxamic acid **16** was prepared

from carboxylic acid **36** following the procedure previously described for **13**.

O-Silylate derivative was purified by flash chromatography on silica gel (*n*-hexane/EtOAc 2:1) to give a yellow oil (51% yield). ¹H NMR (CDCl₃) δ: 0.10 (s, 3H), 0.11 (s, 3H), 0.94 (s, 9H), 1.96–2.05 (m, 2H), 3.50–3.83 (m, 3H), 5.71–5.75 (m, 2H), 7.49–7.61 (m, 4H), 7.77–7.92 (m, 4H).

Hydroxamic acid **16** was obtained as white solid (59% yield) after trituration with *n*-hexane; mp 197–198 °C. ¹H NMR (DMSO-*d*₆) δ: 1.73–1.92 (m, 2H), 3.44–3.53 (m, 2H), 3.64–3.75 (m, 1H), 7.65–7.78 (m, 4H), 7.84 (s, 4H), 8.37–8.42 (m, 2H), 8.89 (s, 1H), 10.61 (br s, 1H). ¹³C NMR (CDCl₃) δ: 30.70, 34.42, 51.89, 122.89, 126.10, 128.30, 131.78, 131.93, 134.18, 140.47, 166.03, 167.70. Anal. (C₁₈H₁₆BrN₃O₆S) C, H, N.

(*R*)-*tert*-Butyl 2-(*N*-(*tert*-Butoxycarbonyl)-2'-(trifluoromethyl)-biphenyl-4-ylsulfonamido)-4-(1,3-dioxoisindolin-2-yl)butanoate (**37**). A solution of aryl bromide **35** (177 mg, 0.28 mmol) in anhydrous dioxane (2.84 mL)/H₂O (0.62 mL) was sequentially treated under nitrogen with K₃PO₄ (138 mg, 0.65 mmol), 2-(trifluoromethyl)phenylboronic acid (59 mg, 0.31 mmol), and Pd(PPh₃)₄ (13.1 mg). The resulting mixture was stirred for 20 min at 85 °C. After being cooled to RT, the mixture was treated with NaHCO₃ and extracted with EtOAc. The combined organic extracts were dried over anhydrous Na₂SO₄, filtered, and evaporated under reduced pressure. The crude was purified by flash chromatography on silica gel column (*n*-hexane/EtOAc 5:1) to give **37** as a yellow solid (139 mg, 71% yield). ¹H NMR (CDCl₃) δ: 1.36 (s, 9H), 1.44 (s, 9H), 2.23–2.38 (m, 1H), 2.63–2.78 (m, 1H), 3.91–3.99 (m, 2H), m (t, 1H), 7.27–7.31 (m, 1H), 7.44–7.49 (m, 2H), 7.53–7.88 (m, 7H), 8.05–8.08 (m, 2H).

(*R*)-4-(1,3-Dioxoisindolin-2-yl)-2-(2'-(trifluoromethyl)biphenyl-4-ylsulfonamido)butanoic Acid (**38**). Carboxylic acid **38** was prepared from *tert*-butyl ester **37** following the procedure previously described for **31**. The crude product was trituted with *n*-hexane and Et₂O to give **38** as a white solid (70% yield). ¹H NMR (DMSO-*d*₆) δ: 1.74–1.88 (m, 1H), 1.95–2.08 (m, 1H), 3.50–3.55 (m, 2H), 3.85–3.95 (m, 1H), 7.40–7.49 (m, 3H), 7.62–7.87 (m, 9H), 8.41–8.45 (m, 2H).

(*R*)-4-(1,3-Dioxoisindolin-2-yl)-*N*-hydroxy-2-(2'-(trifluoromethyl)biphenyl-4-ylsulfonamido)butanamide (**14**). Hydroxamic acid **14** was prepared from carboxylic acid **38** following the procedure previously described for **13**. *O*-Silylate intermediate was purified by flash chromatography on silica gel (*n*-hexane/EtOAc 3:1) to give a yellow oil (85% yield). ¹H NMR (CDCl₃) δ: 0.16 (s, 6H), 0.95 (s, 9H), 1.44 (s, 9H), 2.01–2.07 (m, 2H), 3.49–3.58 (m, 1H), 3.70–3.77 (m, 2H), 5.77–5.81 (m, 2H), 7.32–7.38 (m, 3H), 7.52–7.61 (m, 2H), 7.72–7.88 (m, 7H), 9.39 (s, 1H).

Hydroxamic acid **14** was obtained after trituration with *n*-hexane and Et₂O as a white solid (60% yield); mp 177–178 °C. ¹H NMR (CD₃OD-*d*₄) δ: 1.72–1.91 (m, 1H), 1.94–2.11 (m, 1H), 3.53–3.62 (m, 2H), 3.79–3.85 (m, 1H), 7.41–7.46 (m, 3H), 7.55–7.72 (m, 2H), 7.77–7.92 (m, 7H). ¹³C NMR (CD₃OD-*d*₄) δ: 30.94, 33.87, 52.19, 122.36, 125.40, 125.80, 127.71, 129.13, 131.25, 131.54, 133.54, 139.71, 143.90, 167.70. Anal. (C₂₅H₂₀F₃N₃O₆S) C, H, N.

4-(But-2-ynyloxy)benzenesulfonamide (**40**). To a cooled (0 °C) solution of 4-butyloxybenzene sulfonyl chloride **39** (3.00 g, 11.6 mmol) in CH₃CN (1.16 mL), a solution of aqueous NH₃ 30% (3.71 mL) was added dropwise. The resulting mixture was stirred for 10 min at RT, and then it was diluted with water and extracted with CHCl₃. Organic layers were dried over Na₂SO₄ and concentrated in vacuo to give **40** as a white solid (2.6 g, 94% yield). ¹H NMR (DMSO-*d*₆) δ: 1.83 (t, *J* = 2.2 Hz, 3H), 4.84 (q, *J* = 2.2 Hz, 2H), 7.09–7.13 (m, 2H), 7.23 (br s, 2H), 7.73–7.77 (m, 2H).

tert-Butyl 4-(But-2-ynyloxy)phenylsulfonfylcarbamate (**41**). Sulfonamide **40** (1.6 g, 6.68 mmol) was suspended in dry CH₂Cl₂ (8.35 mL) containing DMAP (81.6 mg, 0.66 mmol) and Et₃N

(1.02 mL, 7.35 mmol). A solution of di-(*tert*-butyl)dicarbonate (1.67 g, 7.69 mmol) in dry CH₂Cl₂ (11.6 mL) was added dropwise, and the mixture was stirred at room temperature overnight. The solution was concentrated in vacuo, and the residue was treated with EtOAc and HCl 1N. The organic phase was then washed with water and brine, dried over Na₂SO₄, and evaporated. The crude product was purified by flash chromatography on silica gel (*n*-hexane/EtOAc 3:1) to afford **41** as a yellow oil (1.75 g, 81% yield). ¹H NMR (CDCl₃) δ: 1.39 (s, 9H), 1.86 (t, *J* = 2.2 Hz, 3H), 4.73 (q, *J* = 2.2 Hz, 2H), 7.04–7.09 (m, 2H), 7.93–7.97 (m, 2H).

General Procedure for the Synthesis of Esters 43–45. DIAD (0.75 mL, 3.82 mmol) was added dropwise to a solution containing the appropriate alcohol **34**, **24**, or **42** (1.53 mmol), Boc-sulfonamide **41** (750 mg, 2.30 mmol), and triphenylphosphine (1.2 g, 4.57 mmol) in anhydrous THF (15.3 mL) under nitrogen atmosphere at 0 °C. The resulting solution was stirred for 4 h at RT and evaporated under reduced pressure.

(*R*)-*tert*-Butyl 2-(4-(But-2-ynyloxy)-*N*-(*tert*-butoxycarbonyl)-phenylsulfonamido)-4-(1,3-dioxoisindolin-2-yl)butanoate (**43**). The title compound was prepared from sulfonamide **41** and alcohol **34** following the general procedure. The crude product was purified by flash chromatography on silica gel (*n*-hexane/EtOAc 3:1) to give a yellow oil (40% yield). ¹H NMR (CDCl₃) δ: 1.38 (s, 9H), 1.41 (s, 9H), 1.85 (t, *J* = 2.2 Hz, 3H), 2.20–2.31 (m, 1H), 2.56–2.66 (m, 1H), 3.90 (t, *J* = 7.14 Hz, 2H), 4.72 (d, *J* = 2.2 Hz, 2H), 5.04 (t, *J* = 7 Hz, 1H), 7.00–7.05 (m, 2H), 7.68–7.72 (m, 2H), 7.81–7.87 (m, 2H), 7.93–7.97 (m, 2H).

(*R*)-*tert*-Butyl 8-(4-(But-2-ynyloxy)phenylsulfonfyl)-11,11-dimethyl-3,9-dioxo-1-phenyl-2,10-dioxo-4,8-diazadodecane-7-carboxylate (**44**). The title compound was prepared from sulfonamide **41** and alcohol **24** following the general procedure. The crude product was purified by flash chromatography on silica gel (*n*-hexane/EtOAc 5:2) to afford **44** as a colorless oil (63% yield). ¹H NMR (CDCl₃) δ: 1.33 (s, 9H), 1.40 (s, 9H), 1.85 (t, *J* = 2.2 Hz, 3H), 2.12–2.21 (m, 1H), 2.34–2.48 (m, 1H), 3.13–3.30 (m, 1H), 3.55–3.66 (m, 1H), 4.73 (q, *J* = 2.2 Hz, 2H), 4.96 (dd, *J*₁ = 4.4 Hz, *J*₂ = 10.7 Hz, 1H), 5.11 (s, 2H), 5.47 (m, 1H), 7.02–7.06 (m, 2H), 7.35 (s, 5H), 7.94–7.99 (m, 2H).

(*R*)-Benzyl 2-(4-(But-2-ynyloxy)-*N*-(*tert*-butoxycarbonyl)-phenylsulfonamido)-4-(1,3-dioxoisindolin-2-yl)butanoate (**45**). The title compound was prepared from sulfonamide **41** and alcohol **42** following the general procedure. The crude product was purified by flash chromatography on silica gel (*n*-hexane/EtOAc 5:2) to afford **45** as a yellow oil (48% yield). ¹H NMR (CDCl₃) δ: 1.29 (s, 9H), 1.85 (s, 3H), 2.28–2.39 (m, 1H), 2.62–2.72 (m, 1H), 3.93 (t, *J* = 7.7 Hz, 2H), 4.64–4.66 (m, 2H), 4.88–5.04 (m, 1H), 5.12 (s, 2H), 6.79–6.83 (m, 2H), 7.20–7.23 (m, 2H), 7.30–7.33 (m, 3H), 7.67–7.72 (m, 2H), 7.83–7.87 (m, 2H).

(*R*)-2-(4-(But-2-ynyloxy)phenylsulfonamido)-4-(1,3-dioxoisindolin-2-yl)butanoic Acid (**46**). Carboxylic acid **46** was prepared from ester **43** following the procedure previously described for **31**.

Carboxylic acid **46** was obtained as a green solid (94% yield). ¹H NMR (DMSO-*d*₆) δ: 1.84 (s, 3H), 1.93–2.08 (m, 2H), 3.56–3.60 (m, 2H), 3.77 (dd, *J*₁ = 8.42 Hz, *J*₂ = 14.46 Hz, 1H), 4.82 (s, 2H), 7.03–7.07 (m, 2H), 7.67–7.72 (m, 2H), 7.80–7.88 (m, 4H), 8.12–8.17 (m, 2H).

(*R*)-2-(4-(But-2-ynyloxy)phenylsulfonamido)-4-(1,3-dioxoisindolin-2-yl)-*N*-hydroxybutanamide (**18**). Hydroxamic acid **18** was prepared from carboxylic acid **46** following the procedure previously described for **13**. *O*-Silylate intermediate was purified by flash chromatography on silica gel (*n*-hexane/EtOAc 3:2) to give a yellow oil (25% yield). ¹H NMR (CDCl₃) δ: 0.12 (d, *J* = 2.56 Hz, 6H), 0.94 (s, 9H), 1.86–1.88 (t, *J* = 2.2 Hz, 3H), 1.99–2.05 (m, 1H), 2.63 (s, 1H), 3.50–3.78 (m, 3H), 4.65–4.68 (d, *J* = 2.2 Hz, 2H), 5.62–5.67 (m, 1H), 6.89–6.93 (d, *J* = 9 Hz, 2H), 7.64–7.68 (d, *J* = 9 Hz, 2H), 7.78–7.90 (m, 4H), 9.38 (br s, 1H). Hydroxamic acid **18** was obtained after

trituration with *n*-hexane and Et₂O as a yellow solid (92% yield); mp 134–135 °C; [α]_D²⁰ −7.8° (*c* 0.06, MeOH). ¹H NMR (DMSO-*d*₆) δ : 1.67–1.75 (m, 2H), 1.83 (s, 3H), 3.40–3.60 (m, 2H), 3.61–3.72 (m, 1H), 4.81 (d, 2H, *J* = 2.2 Hz), 7.03–7.07 (m, 2H), 7.68–7.77 (m, 2H), 7.84 (s, 4H), 8.05–8.1 (m, 1H) 10.60 (s, 1H). ¹³C NMR (CDCl₃) δ : 1.82, 31.38, 33.89, 51.88, 55.76, 88.38, 114.27, 122.20, 128.30, 131.57, 133.43, 143.83, 167.04. Anal. (C₂₂H₂₁N₃O₇S) C, H, N.

(*R*)-4-(Benzyloxycarbonylamino)-2-(4-(but-2-ynoxy)phenylsulfonamido)butanoic Acid (47). Carboxylic acid **47** was prepared from ester **44** following the procedure previously described for **31**.

The purple oil obtained was purified by trituration with *n*-hexane to give the double deprotected carboxylic acid **47** as a white solid (79% yield). ¹H NMR (CDCl₃) δ : 1.85 (t, *J* = 2.2 Hz, 3H), 2.12–2.21 (m, 1H), 2.34–2.45 (m, 1H), 3.13–3.45 (m, 2H), 3.81–3.93 (m, 1H), 4.67 (q, *J* = 2.2 Hz, 2H), 5.09 (s, 2H), 5.39 (m, 1H), 6.57 (m, 1H), 6.97–7.04 (m, 2H), 7.34 (s, 5H), 7.74–7.78 (m, 2H).

(*R*)-Benzyl 3-(4-(But-2-ynoxy)phenylsulfonamido)-4-(hydroxyamino)-4-oxobutylcarbamate (17). Hydroxamic acid **17** was prepared from carboxylic acid **47** following the procedure previously described for **13**. *O*-Silylate intermediate was purified by flash chromatography (*n*-hexane/EtOAc 2:1) using a Isolute Si (II) cartridge to give a yellow oil (43% yield). ¹H NMR (CDCl₃) δ : 0.03 (s, 6H), 0.90 (s, 9H), 1.63 (s, 2H), 1.85 (t, *J* = 2.2 Hz, 3H), 3.07–3.23 (m, 1H), 3.29–3.45 (m, 1H), 3.62–3.74 (m, 1H), 4.65 (q, *J* = 2.2 Hz, 2H), 5.11 (d, *J* = 3.8 Hz, 2H), 5.30–5.38 (m, 1H), 5.80–5.88 (m, 1H), 6.91–6.95 (m, 2H), 7.37 (s, 5H), 7.66–7.70 (m, 2H), 9.77 (s, 1H). Hydroxamic acid **17** was obtained after trituration with *n*-hexane and Et₂O as a white solid (72% yield); mp 148–150 °C; [α]_D²⁰ −4° (*c* 0.1, MeOH). ¹H NMR (DMSO-*d*₆) δ : 1.50–1.66 (m, 2H), 1.83 (t, *J* = 2.2 Hz, 3H), 2.81–2.90 (m, 2H), 3.50–3.60 (m, 1H), 4.82 (s, 2H), 4.99 (s, 2H), 7.05–7.09 (m, 2H), 7.34 (s, 5H), 7.67–7.71 (m, 2H), 7.98–8.02 (m, 1H), 8.90 (br s, 1H), 10.53 (s, 1H). ¹³C NMR (CDCl₃) δ : 3.80, 33.22, 37.19, 56.88, 67.18, 73.17, 84.90, 115.36, 128.03, 128.62, 129.25, 131.40, 136.25, 161.39. Anal. (C₂₂H₂₅N₃O₇S) C, H, N.

(*R*)-Benzyl 2-(4-(But-2-ynoxy)phenylsulfonamido)-4-(1,3-dioxoisindolin-2-yl)butanoate (48). Benzyl ester **48** was obtained by deprotection of Boc-sulfonamide **45** with TFA as described for compounds **46**, **47**. The crude product was purified by flash chromatography (*n*-hexane/EtOAc 4:1) using a Isolute Si (II) cartridge to give **48** as a white solid (63% yield). ¹H NMR (CDCl₃) δ : 1.83 (t, *J* = 2.2 Hz, 3H), 2.09–2.20 (m, 2H), 3.65–3.78 (m, 1H), 3.84–3.98 (m, 1H), 4.03–4.17 (m, 1H), 4.66 (d, *J* = 2.2 Hz, 2H), 4.78 (dd, *J*₁ = 12.09 Hz, *J*₂ = 21.61 Hz, 2H), 5.48 (d, *J* = 9 Hz, 1H), 6.92–6.96 (m, 2H), 7.12–7.17 (m, 2H), 7.29–7.34 (m, 3H), 7.68–7.85 (m, 6H).

(*R*)-Benzyl 2-(4-(But-2-ynoxy)-*N*-isobutylphenylsulfonamido)-4-(1,3-dioxoisindolin-2-yl)butanoate (49). A solution of sulfonamide **48** (248 mg, 0.45 mmol) in anhydrous DMF (7.2 mL) was treated with K₂CO₃ (626 mg, 4.53 mmol) and 1-iodo-2-methyl-propane (0.06 mL, 0.5 mmol). The reaction mixture was stirred for 3 days at room temperature, diluted with H₂O, and extracted with EtOAc. The combined organic extracts were dried over anhydrous Na₂SO₄, filtered, and evaporated under reduced pressure. The crude product was purified by flash chromatography (*n*-hexane/EtOAc 2:1) to afford the isobutyl sulfonamide **49** as a yellow oil (42 mg, 15% yield). ¹H NMR (CDCl₃) δ : 0.73 (d, *J* = 6.5 Hz, 3H), 0.82 (d, *J* = 6.5 Hz, 3H), 1.85 (t, *J* = 2.2 Hz, 3H), 1.96–2.12 (m, 2H), 2.35–2.49 (m, 1H), 2.70–2.81 (m, 1H), 2.93–3.04 (m, 1H), 3.79 (t, *J* = 6.9 Hz, 2H), 4.03–4.17 (m, 1H), 4.65 (d, *J* = 2.2 Hz, 2H), 4.97 (s, 2H), 6.84–6.88 (m, 2H), 7.33–7.35 (m, 5H), 7.65–7.73 (m, 4H), 7.83–7.85 (m, 2H).

(*R*)-2-(4-(But-2-ynoxy)-*N*-isobutylphenylsulfonamido)-4-(1,3-dioxoisindolin-2-yl)butanoic Acid (50). A suspension of benzyl ester **49** (42 mg, 0.07 mmol) and KOH (11.7 mg, 0.21 mmol) in

H₂O (1.0 mL) was heated at 80 °C for 4 h. After being cooled to RT, the reaction was treated with HCl 1N and then extracted with CHCl₃. The organic phase was dried over Na₂SO₄ and concentrated to give **50** as a yellow oil (34 mg, 96% yield). ¹H NMR (CDCl₃) δ : 0.85 (d, *J* = 6.5 Hz, 3H), 0.94 (d, *J* = 6.5 Hz, 3H), 1.85 (t, *J* = 2.2 Hz, 3H), 1.69–2.08 (m, 2H), 2.61–3.21 (m, 4H), 3.77–3.84 (m, 1H), 3.92–4.09 (m, 1H), 4.65 (d, *J* = 2.2 Hz, 2H), 6.91–6.95 (m, 2H), 7.34–7.42 (m, 3H), 7.58–7.75 (m, 3H).

(*R*)-2-(4-(But-2-ynoxy)-*N*-isobutylphenylsulfonamido)-4-(1,3-dioxoisindolin-2-yl)-*N*-hydroxybutanamide (19). Hydroxamic acid **19** was prepared from carboxylic acid **50** following the procedure previously described for **13**. *O*-Silylate intermediate was purified by flash chromatography (*n*-hexane/EtOAc 2:1) to give a colorless oil (40% yield). ¹H NMR (CDCl₃) δ : 0.26 (s, 6H), 0.73 (d, *J* = 6.5 Hz, 3H), 0.83 (d, *J* = 6.5 Hz, 3H), 1.00 (s, 9H), 1.84 (t, *J* = 2.2 Hz, 3H), 1.97–2.07 (m, 2H), 2.35–2.45 (m, 1H), 2.71–2.81 (m, 1H), 2.93–3.04 (m, 1H), 3.80 (t, *J* = 6.9 Hz, 2H), 3.98–4.07 (m, 1H), 4.66 (d, *J* = 2.2 Hz, 2H), 6.84–6.88 (m, 2H), 7.33–7.35 (m, 4H), 7.66–7.70 (m, 2H), 9.08 (s, 1H).

Hydroxamic acid **19** was obtained after a reverse phase chromatography (H₂O/CH₃CN 1:1) as a white solid (55% yield); mp 120–121 °C. ¹H NMR (CDCl₃) δ : 0.95 (d, *J* = 6.5 Hz, 3H), 0.89 (d, *J* = 6.5 Hz, 3H), 1.87 (t, *J* = 2.2 Hz, 3H), 1.95–2.05 (m, 2H), 2.32–2.43 (m, 1H), 3.01–3.46 (m, 4H), 4.06–4.13 (m, 1H), 4.61 (d, *J* = 2.2 Hz, 2H), 6.73–6.77 (m, 2H), 7.56–7.60 (m, 2H), 7.74–7.86 (m, 4H), 9.60 (br s, 1H). ¹³C NMR (CDCl₃) δ : 3.72, 20.65, 23.10, 25.12, 34.26, 49.41, 51.37, 54.45, 80.82, 83.12, 114.63, 128.12, 132.30, 163.81, 168.75, 169.23. Anal. (C₂₆H₂₉N₃O₇S) C, H, N.

(*S*)-Benzyl 4-(1,3-Dioxoisindolin-2-yl)-2-hydroxybutanoate (42). A solution of commercially available carboxylic acid **51** (500 mg, 2.00 mmol) in anhydrous DMF (4.0 mL) was cooled to 0 °C. Cesium carbonate (653 mg, 2.00 mmol) was added, and the mixture was stirred for 30 min at 0 °C. Benzyl bromide (0.24 mL, 2.00 mmol) was added, and the reaction mixture was stirred at 0 °C for 30 min and then at room temperature overnight. The mixture was poured into H₂O and extracted with Et₂O. The combined extracts were washed with H₂O and saturated NaCl, dried over Na₂SO₄, filtered, and evaporated under reduced pressure to afford **42** (571 mg, 84% yield) as a yellow oil that was utilized in the next step without further purification. ¹H NMR (CDCl₃) δ : 1.99–2.26 (m, 2H), 3.06 (d, *J* = 5.5 Hz, 1H), 3.85–3.93 (m, 2H), 4.23–4.31 (m, 1H), 5.13 (d, *J* = 3.3 Hz, 2H), 7.34 (s, 5H), 7.69–7.76 (m, 2H), 7.81–7.86 (m, 2H).

MMPs and ADAMs Inhibition Assays.⁴⁸ Recombinant human MMP-14 catalytic domain was a kind gift of Prof. Gillian Murphy (Department of Oncology, University of Cambridge, UK). Pro-MMP-1, pro-MMP-2, pro-MMP-9, and recombinant human ADAM-17 (PF133) were purchased from Calbiochem. Recombinant human ADAM-10 was purchased from R&D Systems. Pro-enzymes were activated immediately prior to use with *p*-aminophenylmercuric acetate (APMA 2 mM for 1 h at 37 °C for MMP-2, APMA 2 mM for 2 h at 37 °C for MMP-1 and 1 mM for 1 h at 37 °C for MMP-9). For assay measurements, the inhibitor stock solutions (DMSO, 10 mM) were further diluted at seven different concentrations for each MMP in the fluorometric assay buffer (FAB: Tris 50 mM, pH = 7.5, NaCl 150 mM, CaCl₂ 10 mM, Brij-35 0.05%, and DMSO 1%). Activated enzyme (final concentration 0.56 nM for MMP-2, 1.3 nM for MMP-9, 1.0 nM for MMP-14 cd, 2.0 nM for MMP-1, 5 nM for ADAM-17 and 20 nM for ADAM-10) and inhibitor solutions were incubated in the assay buffer for 4 h at 25 °C. ADAM-17 was incubated for 30 min at 37 °C and ADAM-10 for 1 h at 37 °C in a different buffer at pH = 9 (Tris 25 mM, ZnCl₂ 25 μ M, Brij-35 0.005%). After the addition of 200 μ M solution of the fluorogenic substrate Mca-Lys-Pro-Leu-Gly-Leu-Dap(Dnp)-Ala-Arg-NH₂⁴⁹ (Bachem) for all the enzymes in DMSO (final concentration 2 μ M for all enzymes, 10 μ M for ADAM-10), the hydrolysis was monitored every 15 s for 20 min, recording the increase in fluorescence (λ_{ex} = 325 nm, λ_{em} = 395 nm) with a

Molecular Devices SpectraMax Gemini XS plate reader. The assays were performed in duplicate in a total volume of 200 μ L per well in 96-well microtiter plates (Corning black, NBS). Control wells lack inhibitor. The MMP inhibition activity was expressed in relative fluorescent units (RFU). Percent of inhibition was calculated from control reactions without the inhibitor. IC_{50} was determined using the formula: $V_i/V_o = 1/(1 + [I]/IC_{50})$, where V_i is the initial velocity of substrate cleavage in the presence of the inhibitor at concentration $[I]$ and V_o is the initial velocity in the absence of the inhibitor. Results were analyzed using SoftMax Pro software⁵⁰ and GraFit software.⁵¹

Cells and Reagents. Human epithelial ovarian cancer (EOC) cell lines SKOV3 (ATCC, Manassas, VA) and A2774 (from J. Bénard, Institut Gustave Roussy, Paris, France), neuroblastoma (NB) cell line GI-CA-N (established at the Laboratory of Oncology, Gaslini Institute, Genoa, Italy), and breast cancer cell lines MCF7 and MDA-MB-468 (ATCC) were grown in RPMI 1640 supplemented with 10% heat-inactivated fetal calf serum (FCS), 2 mM glutamine, and penicillin–streptomycin (100 μ g/mL) (BioWhittaker Cambrex, Verviers, Belgium) at 37 °C in a 5% CO₂ incubator.

Chemicals were from Sigma Chemical Co. (St. Louis, MO). Pervanadate (PV) was freshly prepared for each experiment by mixing sodium orthovanadate (0.1 M) and H₂O₂ (0.1 M) and was used within 20 min of preparation. Recombinant human EGF was purchased from PeptoTech EC (London, UK). Metalloproteinase inhibitors were dissolved in DMSO as 10 mM stock solution and stored in aliquots at –20 °C.

Cell Treatments and ELISA. To assess the shedding of the ALCAM molecule, subconfluent cells were cultured in 24-well plates in medium 0.1% FCS plus the indicated concentration of protease inhibitors or the equivalent amount of their solvent. Assays were performed in duplicate. After 30 min at 37 °C, 200 μ M pervanadate or 100 ng/mL EGF was added and incubation prolonged for the indicated times. Untreated and treated conditioned media were then collected, centrifuged at 1000g and used undiluted for sALCAM detection by an ELISA assay (DuoSet ELISA Development kit, R&D System). Each sample was tested in duplicate, and background values were subtracted. Data were expressed as the mean \pm SD and were analyzed using a two-tailed Student's *t* test.

MTT Assay. Cell viability after treatment with the different inhibitors was evaluated by a microculture tetrazolium reduction assay using MTT [3-(4,5-dimethylthiazol-2-yl) 2,5-diphenyl-tetrazolium bromide; Sigma]. Briefly, 2×10^3 cells per well were seeded in 96-microwell flat-bottom plates and incubated with various concentrations of compounds for 24, 48, or 72 h at 37 °C. Then 20 μ L of MTT stock solution (2 mg/mL in PBS) were added to 200 μ L cell cultures for an additional 4 h of incubation. MTT-containing culture medium was then removed, and precipitated formazan was dissolved in 100 μ L of DMSO. Results were read within 15 min in a microplate reader spectrometer at 540 nm (MEDGENIX 400 ATC, Medgenix Diagnostics, Fleurus, Belgium), and the means of triplicates were calculated. Cell survival was expressed as percentage of control samples.

Docking Simulations. Molecular docking of **17** into the X-ray structures of TACE (PDB codes: 2I47, 2FV5, 2OI0, 3EWJ, 2DDF) was carried out using the Glide 5.5 program.⁵² Maestro 9.0.211⁵³ was employed as the graphical user interface, and Figure 3 representing the most probable binding mode of **17** was rendered by the Chimera software package.⁵⁴

Ligand and Protein Setup. The inhibitor structure was first generated through the Dundee PRODRG2 Server.⁵⁵ Then, a geometry optimized ligand was prepared using Lig-Prep 2.3 as implemented in Maestro. The target proteins were prepared using the protein preparation wizard in Maestro 9.0.211. Water molecules were removed, and the resulting proteins were aligned based on the α -carbon trace. Hydrogen atoms were added, a +2 charge was assigned to the zinc ion in the active site, and

minimization was performed until the rmsd of all heavy atoms was within 0.3 Å of the crystallographic positions. The binding pocket was identified by placing a 20 Å cube around the catalytic ion. All proteins were then processed through the Protein Preparation Wizard of the graphical user interface Maestro and the OPLS-2001 force field.

Docking Setting. Molecular docking calculations were performed with the aid of Glide 5.5 in extra-precision (XP)^{56,57} mode, using Glidescore for ligand ranking. A constraint that forced the interaction with the metal ion was included.

Molecular Dynamics Simulations. The two binding poses obtained for **17** as a result of the docking calculations in the 2DDF crystal structure were subjected to an MD simulation by means of AMBER 9.0 package software.⁵⁸ Ligand force-field parameters were derived using the Antechamber program,⁵⁹ and partial charges for the inhibitor were derived using the AM1-BCC procedure in Antechamber. For the zinc atom, a ion parametrization based on quantum chemistry calculations as suggested by Cheng et al.⁶⁰ was used. The complex was inserted in a box of TIP3P⁶¹ pre-equilibrated water molecules. Then, an appropriate number of Na⁺ ions were randomly placed by means of the add ions routine of Xleap to maintain the neutrality of the system. First, water molecules and counterions were energy minimized using steepest descent followed by conjugated gradient. Second, a minimization of the entire system was performed by means of 2000 steps of steepest descent followed by 3000 steps of conjugated gradient. Equilibration runs were carried out by heating the system to 300 K in 1 ns. This was followed by 10 ns MD simulations in the NPT ensemble (constant temperature and pressure). The parm99⁶² version of the all-atom Amber force field⁶³ was used for the protein and the counterions. van der Waals and short-range electrostatic interactions were estimated within a 8 Å cutoff, whereas the long-range electrostatic interactions were assessed by using the particle mesh Ewald (PME) method,⁶⁴ with a 1 Å charge grid spacing interpolated by a fourth-order B-spline, and by setting the direct sum tolerance to 10^{–5}. Bonds involving hydrogen atoms were constrained by using the SHAKE algorithm⁶⁵ with a relative geometric tolerance for coordinate resetting of 0.00001 Å. Berendsen's coupling algorithms⁶⁶ were employed to maintain constant temperature and pressure with the same scaling factor for both solvent and solutes and with the time constant for heat bath coupling maintained at 1.5 ps. The pressure for the isothermal–isobaric ensemble was regulated by using a pressure relaxation time of 1 ps in Berendsen's algorithm. The simulations of the solvated protein models were performed using a constant pressure of 1 atm and a constant temperature of 300 K. Analysis of MD trajectories was attained using the ptraj software.⁶⁷ All calculations were performed on a Linux machine employing a Fedora Core 7 architecture.

Acknowledgment. We are grateful for financial support given by MIUR (Prin 2007), by Cofinanziamento di Ateneo 2007 Università di Pisa, by Compagnia di SanPaolo, by AIRC and by Ministero della Salute.

Supporting Information Available: Experimental procedure to prepare compounds **10–12**, criteria to select TACE X-ray structures for docking studies, rmsd plots of **17** in the binding mode A and B, picture representing the superimposition of frames from MD simulation, and a table reporting the HPLC purity analysis and the combustion analysis data of the final products. This material is available free of charge via the Internet at <http://pubs.acs.org>.

References

- (1) Arribas, J.; Bech-Serra, J. J.; Santiago-Josefat, B. ADAMs, cell migration and cancer. *Cancer Metastasis Rev.* **2006**, *25*, 57–68.

- (2) Mochizuki, S.; Okada, Y. ADAMs in cancer cell proliferation and progression. *Cancer Sci.* **2007**, *98*, 621–628.
- (3) Dong, J.; Opreko, L. K.; Dempsey, P. J.; Lauffenburger, D. A.; Coffey, R. J.; Wiley, H. S. Metalloprotease-mediated ligand release regulates autocrine signaling through the epidermal growth factor receptor. *Proc. Natl. Acad. Sci. U.S.A.* **1999**, *96*, 6235–6240.
- (4) Garton, K. J.; Gough, P. J.; Raines, E. W. Emerging roles for ectodomain shedding in the regulation of inflammatory responses. *J. Leukocyte Biol.* **2006**, *79*, 1105–1116.
- (5) Swart, G. W. M. Activated leukocyte cell adhesion molecule (CD166/ALCAM): Developmental and mechanistic aspects of cell clustering and cell migration. *Eur. J. Cell Biol.* **2002**, *81*, 313–321.
- (6) Nelissen, J. M. D. T.; Peters, I. M.; De Grooth, B. G.; Van Kooyk, Y.; Figdor, C. G. Dynamic regulation of activated leukocyte cell adhesion molecule-mediated homotypic cell adhesion through the actin cytoskeleton. *Mol. Biol. Cell* **2000**, *11*, 2057–2068.
- (7) Zimmerman, A. W.; Nelissen, J. M.; van Emst-de Vries, S. E.; Willems, P. H.; de Lange, F.; Collard, J. G.; van Leeuwen, F. N.; Figdor, C. G. Cytoskeletal restraints regulate homotypic ALCAM-mediated adhesion through PKC α independently of Rho-like GTPases. *J. Cell. Sci.* **2004**, *117*, 2841–2852.
- (8) Swart, G. W.; Lunter, P. C.; Kilsdonk, J. W.; Kempen, L. C. Activated leukocyte cell adhesion molecule (ALCAM/CD166): signaling at the divide of melanoma cell clustering and cell migration? *Cancer Metastasis Rev.* **2005**, *24*, 223–236.
- (9) Bogenrieder, T.; Herlyn, M. Axis of evil: molecular mechanisms of cancer metastasis. *Oncogene*. **2003**, *22*, 6524–6536.
- (10) Rosenthal, E. L.; Matrisian, L. M. Matrix metalloproteases in head and neck cancer. *Head Neck* **2006**, *28*, 639–648.
- (11) (a) Uchida, N.; Yang, Z.; Combs, J.; Pourquie, O.; Nguyen, M.; Ramanathan, R.; Fu, J.; Welply, A.; Chen, S.; Weddell, G.; Sharma, A. K.; Leiby, K. R.; Karagogeos, D.; Hill, B.; Humeau, L.; Stallcup, W. B.; Hoffman, R.; Tsukamoto, A. S.; Gearing, D. P.; Péault, B. The characterization, molecular cloning and expression of a novel hematopoietic cell antigen from CD34+ human bone marrow cells. *Blood* **1997**, *89*, 2706–2716. (b) Van Kempen, L. C.; Nelissen, J. M.; Degen, W. G.; Torensma, R.; Weidle, U. H.; Bloemers, H. P.; Figdor, C. G.; Swart, G. W. Molecular basis for the homophilic activated leukocyte cell adhesion molecule (ALCAM)–ALCAM interaction. *J. Biol. Chem.* **2001**, *276*, 25783–25790.
- (12) Ofori-Acquah, S. F.; King, J. A. Activated leukocyte cell adhesion molecule: a new paradox in cancer. *Transl. Res.* **2008**, *151*, 122–128.
- (13) Piazza, T.; Cha, E.; Bongarzone, I.; Canevari, S.; Bolognesi, A.; Polito, L.; Bargellesi, A.; Sassi, F.; Ferrini, S.; Fabbri, M. Internalization and recycling of ALCAM/CD166 detected by a fully human single chain recombinant antibody. *J. Cell Sci.* **2005**, *118*, 1515–1525.
- (14) Rosso, O.; Piazza, T.; Bongarzone, I.; Rossello, A.; Mezzanzanica, D.; Canevari, S.; Orenco, A. M.; Puppo, A.; Ferrini, S.; Fabbri, M. The ALCAM shedding by the metalloprotease ADAM17/TACE is a tyrosine kinase-inducible process involved in motility of ovarian carcinoma cells. *Mol. Cancer Res.* **2007**, *5*, 1246–1253.
- (15) MacPherson, L. J.; Bayburt, E. K.; Capparelli, M. P.; Carroll, B. J.; Goldstein, R.; Justice, M. R.; Zhu, L. J.; Hu, S. I.; Melton, R. A.; Fryer, L.; Goldberg, R. L.; Dougherty, J. R.; Spirito, S.; Blancuzzi, V.; Wilson, D.; O'Byrne, E. M.; Ganu, V.; Parker, D. T. Discovery of CGS 27023A, a non-peptidic, potent, and orally active stromelysin inhibitor that blocks cartilage degradation in rabbits. *J. Med. Chem.* **1997**, *40*, 2525–2532.
- (16) Mezzanzanica, D.; Fabbri, M.; Bagnoli, M.; Staurengo, S.; Losa, M.; Balladore, E.; Alberti, P.; Lusa, L.; Ditto, A.; Ferrini, S.; Pierotti, M. A.; Barbareschi, M.; Pilotti, S.; Canevari, S. Subcellular localization of activated cell adhesion molecule is a molecular predictor of survival in ovarian carcinoma patients. *Clin. Cancer Res.* **2008**, *14*, 1726–1733.
- (17) Bech-Serra, J. J.; Santiago-Josefat, B.; Esselens, C.; Saftig, P.; Baselga, J.; Arribas, J.; Canals, F. Proteomic Identification of Desmoglein 2 and Activated Leukocyte Cell Adhesion Molecule as Substrates of ADAM17 and ADAM10 by Difference Gel Electrophoresis. *Mol. Cell Biol.* **2006**, *26*, 5086–5095.
- (18) Maretzky, T.; Schulte, M.; Ludwig, A.; Rose-John, S.; Blobel, C.; Hartmann, D.; Altevogt, P.; Saftig, P.; Reiss, K. L1 is sequentially processed by two differently activated metalloproteases and presenilin/gamma-secretase and regulates neural cell adhesion, cell migration, and neurite outgrowth. *Mol. Cell Biol.* **2005**, *25*, 9040–9045.
- (19) Santiago-Josefat, B.; Esselens, C.; Bech-Serra, J. J.; Arribas, J. Post-transcriptional up-regulation of ADAM17 upon epidermal growth factor receptor activation and in breast tumors. *J. Biol. Chem.* **2007**, *282*, 8325–8331.
- (20) Pruessmeyer, J.; Ludwig, A. The good, the bad and the ugly substrates for ADAM10 and ADAM17 in brain pathology, inflammation and cancer. *Semin. Cell Dev. Biol.* **2009**, *20*, 164–174.
- (21) Rossello, A.; Nuti, E. Drug design of sulfonfylated MMP inhibitors. In *Drug Design of Zinc-Enzyme Inhibitors: Functional, Structural, and Disease Applications*; Wiley Series in Drug Discovery and Development; Wang, B., series Ed.; John Wiley & Sons, Inc.: New York, 2009; pp 549–589.
- (22) Tamura, Y.; Watanabe, F.; Nakatani, T.; Yasui, K.; Fuji, M.; Komurasaki, T.; Tsuzuki, H.; Maekawa, R.; Yoshioka, T.; Kawada, K.; Sugita, K.; Ohtani, M. Highly selective and orally active inhibitors of type IV collagenase (MMP-9 and MMP-2): *N*-sulfonfylamino acid derivatives. *J. Med. Chem.* **1998**, *41*, 640–649.
- (23) O'Brien, P. M.; Ortwine, D. F.; Pavlovsky, A. G.; Picard, J. A.; Sliskovic, D. R.; Roth, B. D.; Dyer, R. D.; Johnson, L. L.; Man, C. F.; Hallak, H. Structure–activity relationships and pharmacokinetic analysis for a series of potent, systemically available biphenylsulfonamide matrix metalloproteinase inhibitors. *J. Med. Chem.* **2000**, *43*, 156–166.
- (24) Rossello, A.; Nuti, E.; Orlandini, E.; Carelli, P.; Rapposelli, S.; Macchia, M.; Minutolo, F.; Carbonaro, L.; Albini, A.; Benelli, R.; Cercignani, G.; Murphy, G.; Balsamo, A. New *N*-arylsulfonfyl-*N*-alkoxyaminoacetohydroxamic acids as selective inhibitors of gelatinase A (MMP-2). *Bioorg. Med. Chem.* **2004**, *12*, 2441–2450.
- (25) (a) Rossello, A.; Nuti, E.; Carelli, P.; Orlandini, E.; Macchia, M.; Nencetti, S.; Zandomeneghi, M.; Balzano, F.; Uccello Barretta, G.; Albini, A.; Benelli, R.; Cercignani, G.; Murphy, G.; Balsamo, A. *N*-*i*-Propoxy-*N*-biphenylsulfonfylaminobutylhydroxamic acids as potent and selective inhibitors of MMP-2 and MT1-MMP. *Bioorg. Med. Chem. Lett.* **2005**, *15*, 1321–1326. (b) Nuti, E.; Casalini, F.; Avramova, S. I.; Santamaria, S.; Cercignani, G.; Marinelli, L.; La Pietra, V.; Novellino, E.; Orlandini, E.; Nencetti, S.; Tuccinardi, T.; Martinelli, A.; Lim, N.-H.; Visse, R.; Nagase, H.; Rossello, A. *N*-O-Isopropyl Sulfonamido-Based Hydroxamates: Design, Synthesis and Biological Evaluation of Selective Matrix Metalloproteinase-13 Inhibitors as Potential Therapeutic Agents for Osteoarthritis. *J. Med. Chem.* **2009**, *52*, 4757–4773.
- (26) Regarding the debate on the use of hydroxamates as ZBG for metalloenzymes see: (a) Nuti, E.; Panelli, L.; Casalini, F.; Avramova, S. I.; Orlandini, E.; Santamaria, S.; Nencetti, S.; Tuccinardi, T.; Martinelli, A.; Cercignani, G.; D'Amelio, N.; Maiocchi, A.; Uggeri, F.; Rossello, A. Design, Synthesis, Biological Evaluation and NMR Studies of a New Series of Arylsulfones As Selective and Potent Matrix Metalloproteinase-12 Inhibitors. *J. Med. Chem.* **2009**, *52*, 6347–6361. (b) Flipo, M.; Charton, J.; Hocine, A.; Dassonneville, S.; Deprez, B.; Deprez-Poulain, R. Hydroxamates: Relationships between Structure and Plasma Stability. *J. Med. Chem.* **2009**, *52*, 6790–6802.
- (27) Overall, C. M.; Kleifeld, O. Validating matrix metalloproteinases as drug targets and antitargets for cancer therapy. *Nat. Rev. Cancer* **2006**, *6*, 227–239.
- (28) Bertini, I.; Calderone, V.; Fragai, M.; Giachetti, A.; Locante, M.; Luchinat, C.; Maletta, M.; Nativi, C.; Yeo, K. J. Exploring the subtleties of drug–receptor interactions: the case of matrix metalloproteinases. *J. Am. Chem. Soc.* **2007**, *129*, 2466–2475.
- (29) Corrias, M. V.; Gambini, C.; Gregorio, A.; Croce, M.; Barisione, G.; Cossu, C.; Rossello, A.; Ferrini, S.; Fabbri, M. Different subcellular localization of ALCAM molecules in neuroblastoma: association with relapse. *Cell. Oncol.*, accepted for publication.
- (30) Rossello, A.; Nuti, E.; Orlandini, E.; Balsamo, A.; Tuccinardi, T. Compounds having aryl-sulphonamidic structure useful as metalloproteinase inhibitors. Patent WO2008113756, **2008**.
- (31) (a) Rossello, A.; Nuti, E.; Maresca, A. ADAMs and ADAMTs Selective Synthetic Inhibitors. In *Drug Design of Zinc-Enzyme Inhibitors: Functional, Structural, and Disease Applications*; Wiley Series in Drug Discovery and Development; Wang, B., series Ed.; John Wiley & Sons, Inc.: New York, 2009; pp 591–645; (b) Fisher, J. F.; Mobashery, S. Recent advances in MMP inhibitor design. *Cancer Metastasis Rev.* **2006**, *25*, 115–136. (c) Georgiadis, D.; Yiotakis, A. Specific targeting of metzincin family members with small-molecule inhibitors: progress toward a multifarious challenge. *Bioorg. Med. Chem.* **2008**, *16*, 8781–8794.
- (32) (a) Kimura, T.; Miyazaki, S.; Ueda, K.; Tanzawa, K.; Ushiyama, S.; Takasaki, W. Sulfonamide derivatives. Patent WO 9951572 A1, **1999**. (b) Kukkola, P. J.; Robinson, L. A.; Nakajima, M.; Sakaki, J. Sulfonfylamino acid and sulfonfylamino hydroxamic acid derivatives. U.S. Patent US 6277987 B1, **2001**. (c) Heintz, R. M.; Getman, D. P.; McDonald, J. J.; DeCrescenzo, J. A.; Howard, S. Amidoaromatic ring sulfonamide hydroxamic acid compounds. Patent WO 9839329 A1, **1998**. (d) Levin, J. I.; Chen, J. M.; Cole, D. C. Acetylenic α -amino acid-based sulfonamide hydroxamic acid TACE inhibitors. Patent WO 0044709 A2, **2000**. (e) Levin, J. I.; Chen, J. M.; Cole, D. C.;

- Du, M. T.; Laakso, L. M. Acetylenic α -amino acid-based sulfonamide hydroxamic acid TACE inhibitors. U.S. Patent US 6225311 B1, **2001**.
- (33) Rossello, A.; Nuti, E.; Casalini, F.; Fabbì, M.; Ferrini, S. Inibitori di ADAM17 atti a modulare il rilascio di ALCAM (CD166) solubile in cellule tumorali e loro uso nel trattamento terapeutico del carcinoma ovarico epiteliale (EOC). Italian Patent Application TO2009A000648, **2009**.
- (34) Nuti, E.; Orlandini, E.; Nencetti, S.; Rossello, A.; Innocenti, A.; Scozzafava, A.; Supuran, C. T. Carbonic anhydrase and matrix metalloproteinase inhibitors. Inhibition of human tumor-associated isozymes IX and cytosolic isozyme I and II with sulfonated hydroxamates. *Bioorg. Med. Chem.* **2007**, *15*, 2298–2311.
- (35) Neustadt, B. R. Facile Preparation of *N*-(Sulfonyl)carbamates. *Tetrahedron Lett.* **1994**, *35*, 379–380.
- (36) Miyaura, N.; Suzuki, A. Palladium-Catalyzed Cross-Coupling Reactions of Organoboron Compounds. *Chem. Rev.* **1995**, *95*, 2457–2483.
- (37) Levin, J. I.; Chen, J. M.; Cheung, K.; Cole, D.; Crago, C.; Santos, E. D.; Du, X.; Khafizova, G.; MacEwan, G.; Niu, C.; Salaski, E. J.; Zask, A.; Cummons, T.; Sung, A.; Xu, J.; Zhang, Y.; Xu, W.; Ayrar-Kaloustian, S.; Jin, G.; Cowling, R.; Barone, D.; Mohler, K. M.; Black, R. A.; Skotnicki, J. S. Acetylenic TACE inhibitors. Part I. SAR of the acyclic sulfonamide hydroxamates. *Bioorg. Med. Chem. Lett.* **2003**, *13*, 2799–2803.
- (38) (a) Crawford, H. C.; Dempsey, P. J.; Brown, G.; Adam, L.; Moss, M. L. ADAM10 as a therapeutic target for cancer and inflammation. *Curr. Pharm. Des.* **2009**, *15*, 2288–2299. (b) Moss, M. L.; Stoeck, A.; Yan, W.; Dempsey, P. J. ADAM10 as a target for anti-cancer therapy. *Curr. Pharm. Biotechnol.* **2008**, *9*, 2–8.
- (39) Huang, A.; Joseph-McCarthy, D.; Lovering, F.; Sun, L.; Wang, W.; Xu, W.; Zhu, Y.; Cui, J.; Zhang, Y.; Levin, J. I. Structure-based design of TACE selective inhibitors: manipulations in the S1'–S3' pocket. *Bioorg. Med. Chem.* **2007**, *15*, 6170–6181.
- (40) Zatovicova, M.; Sedlakova, O.; Svastova, E.; Ohradanova, A.; Ciampor, F.; Arribas, J.; Pastorek, J.; Pastorekova, S. Ectodomain shedding of the hypoxia-induced carbonic anhydrase IX is a metalloprotease-dependent process regulated by TACE/ADAM17. *Br. J. Cancer* **2005**, *93*, 1267–1276.
- (41) Codony-Servat, J.; Albanell, J.; Lopez-Talavera, J. C.; Arribas, J.; Baselga, K. C. EGF/ErBB receptor family is a pervanadate-activable process that is inhibited by the tissue inhibitor of metalloproteinases-1 in breast cancer cells. *Cancer Res.* **1999**, *59*, 1196–1201.
- (42) Mailhe, N. J.; Baron, A. T.; Barrette, B. A.; Boardman, C. H.; Christensen, T. A.; Cora, E. M.; Faupel-Badger, J. M.; Greenwood, T.; Juneja, S. C.; Lafky, J. M.; Lee, H.; Reiter, J. L.; Podratz, K. C. EGF/ErBB receptor family in ovarian cancer. *Cancer Treat. Res.* **2002**, *107*, 247–258.
- (43) Condon, J. S.; Joseph-McCarthy, D.; Levin, J. I.; Lombart, H. G.; Lovering, F. E.; Sun, L.; Wang, W.; Xu, W.; Zhang, Y. Identification of potent and selective TACE inhibitors via the S1 pocket. *Bioorg. Med. Chem. Lett.* **2007**, *17*, 34–39.
- (44) Mazzola, R. D., Jr.; Zhu, Z.; Sinning, L.; McKittrick, B.; Lavey, B.; Spitler, J.; Kozlowski, J.; Neng-Yang, S.; Zhou, G.; Guo, Z.; Orth, P.; Madison, V.; Sun, J.; Lundell, D.; Niu, X. Discovery of novel hydroxamates as highly potent tumor necrosis factor- α converting enzyme inhibitors. Part II: optimization of the S3' pocket. *Bioorg. Med. Chem. Lett.* **2008**, *18*, 5809–5814.
- (45) Guo, Z.; Orth, P.; Wong, S. C.; Lavey, B. J.; Shih, N. Y.; Niu, X.; Lundell, D. J.; Madison, V.; Kozlowski, J. A. Discovery of novel spirocyclopropyl hydroxamate and carboxylate compounds as TACE inhibitors. *Bioorg. Med. Chem. Lett.* **2009**, *19*, 54–57.
- (46) Ingram, R. N.; Orth, P.; Strickland, C. L.; Le, H. V.; Madison, V.; Beyer, B. M. Stabilization of the autolysis of TNF- α converting enzyme (TACE) results in a novel crystal form suitable for structure-based drug design studies. *Protein Eng. Des. Sel.* **2006**, *19*, 155–161.
- (47) Govinda Rao, B.; Bandarage, U. K.; Wang, T.; Come, J. H.; Perola, E.; Wei, Y.; Tian, S. K.; Saunders, J. O. Novel thiol-based TACE inhibitors: rational design, synthesis, and SAR of thiol-containing aryl sulfonamides. *Bioorg. Med. Chem. Lett.* **2007**, *17*, 2250–2253.
- (48) Knight, C. G.; Willenbrock, F.; Murphy, G. A novel coumarin-labelled peptide for sensitive continuous assays of the matrix metalloproteinases. *FEBS Lett.* **1992**, *296*, 263–266.
- (49) Neumann, U.; Kubota, H.; Frei, K.; Ganu, V.; Leppert, D. Characterization of Mca-Lys-Pro-Leu-Gly-Leu-Dpa-Ala-Arg-NH₂, a fluorogenic substrate with increased specificity constants for collagenases and tumor necrosis factor converting enzyme. *Anal. Biochem.* **2004**, *328*, 166–173.
- (50) *SoftMax Pro 4.7.1*; Molecular Devices: Sunnyvale, CA, **2004**.
- (51) *GraFit version 4*; Erithecus Software: Horley, UK, **1998**.
- (52) *Glide, version 5.5*; Schrödinger, LLC: New York, **2009**.
- (53) *Maestro, version 9.0.211*; Schrödinger, L.L.C.: New York, **2009**.
- (54) Pettersen, E. F.; Goddard, T. D.; Huang, C. C.; Couch, G. S.; Greenblatt, D. M.; Meng, E. C.; Ferrin, T. E. UCSF Chimera—A Visualization System for Exploratory Research and Analysis. *J. Comput. Chem.* **2004**, *25*, 1605–1612.
- (55) Schüttelkopf, A. W.; van Aalten, D. M. PRODRG: a tool for high-throughput crystallography of protein–ligand complexes. *Acta Crystallogr., Sect. D: Biol. Crystallogr.* **2004**, *60*, 1355–1363.
- (56) Friesner, R. A.; Banks, J. L.; Murphy, R. B.; Halgren, T. A.; Klicic, J. J.; Mainz, D. T.; Repasky, M. P.; Knoll, E. H.; Shelley, M.; Perry, J. K.; Shaw, D. E.; Francis, P.; Shenkin, P. S. Glide: A new approach for rapid, accurate docking and scoring. 1. Method and assessment of docking accuracy. *J. Med. Chem.* **2004**, *47*, 1739–1749.
- (57) Friesner, R. A.; Murphy, R. B.; Repasky, M. P.; Frye, L. L.; Greenwood, J. R.; Halgren, T. A.; Sanschagrin, P. C.; Mainz, D. T. Extra Precision Glide: Docking and Scoring Incorporating a Model of Hydrophobic Enclosure for Protein–Ligand Complexes. *J. Med. Chem.* **2006**, *49*, 6177–6196.
- (58) Case, D. A.; Darden, T. E.; Cheatham, T. E. I.; Simmerling, C. L.; Wang, J.; Duke, R. E.; Luo, R.; Merz, K. M.; Wang, B.; Pearlman, D. A.; Crowley, M.; Brozell, S.; Tsui, V.; Gohlke, H.; Mongan, J.; Hornak, V.; Cui, G.; Beroza, P.; Schafmeister, C.; Caldwell, J. W.; Ross, W. S.; Kollman, P. A. *AMBER 9*; University of California: San Francisco, 2006.
- (59) Wang, J.; Wolf, R. M.; Caldwell, J. W.; Kollman, P. A.; Case, D. A. Development and Testing of a General Amber Force Field. *J. Comput. Chem.* **2004**, *25*, 1157–1174.
- (60) Cheng, F.; Zhang, R.; Luo, X.; Shen, J.; Li, X.; Gu, J.; Zhu, W.; Shen, J.; Sagi, I.; Ji, R.; Chen, K.; Jiang, H. Quantum Chemistry Study on the Interaction of the Exogenous Ligands and the Catalytic Zinc Ion in Matrix Metalloproteinases. *J. Phys. Chem. B* **2002**, *106*, 4552–4559.
- (61) Jorgensen, W. L.; Chandrasekhar, J.; Madura, J. D.; Impey, R. W.; Klein, L. M. Comparison of Simple Potential Functions for Simulating Liquid Water. *J. Chem. Phys.* **1983**, *79*, 926–935.
- (62) Wang, J.; Cieplak, P.; Kollman, P. A. How Well Does a Restrained Electrostatic Potential (RESP) Model Perform in Calculating Conformational Energies of Organic and Biological Molecules. *J. Comput. Chem.* **2000**, *21*, 1049–1074.
- (63) Cornell, W. D.; Cieplak, P.; Bayly, C. I.; Gould, I. R.; Merz, K. M.; Ferguson, D. M.; Spellmeyer, D. C.; Fox, T.; Caldwell, J. W.; Kollman, P. A. A Second Generation Force Field for the Simulation of Proteins, Nucleic Acids, and Organic Molecules. *J. Am. Chem. Soc.* **1995**, *117*, 5179–5197.
- (64) Essmann, U.; Perera, L.; Berkowitz, M. L.; Darden, T.; Lee, H.; Pedersen, L. G. A Smooth Particle Mesh Ewald Method. *J. Chem. Phys.* **1995**, *103*, 8577–8593.
- (65) Ryckaert, J. P.; Cicotti, G.; Berendsen, H. J. C. Numerical Integration of the Cartesian Equations of Motion of a System with Constraints: Molecular Dynamics of *n*-Alkanes. *J. Comput. Phys.* **1977**, *23*, 327–341.
- (66) Berendsen, H. J. C.; Postma, J. P. M.; Van Gunsteren, W. F.; Di Nola, A.; Haak, J. R. Molecular Dynamics with Coupling to an External Bath. *J. Chem. Phys.* **1984**, *81*, 3684–3690.
- (67) Shao, J.; Tanner, S. W.; Thompson, N.; Cheatham, T. E. I. Clustering Molecular Dynamics Trajectories: I. Characterizing the Performance of Different Clustering Algorithms. *J. Chem. Theory Comput.* **2007**, *3*, 2312–2334.